General Disclaimer

One or more of the Following Statements may affect this Document

- This document has been reproduced from the best copy furnished by the organizational source. It is being released in the interest of making available as much information as possible.

- This document may contain data, which exceeds the sheet parameters. It was furnished in this condition by the organizational source and is the best copy available.

- This document may contain tone-on-tone or color graphs, charts and/or pictures, which have been reproduced in black and white.

- This document is paginated as submitted by the original source.

- Portions of this document are not fully legible due to the historical nature of some of the material. However, it is the best reproduction available from the original submission.

OLD DOMINION UNIVERSITY RESEARCH FOUNDATION

SCHOOL OF ENGINEERING
OLD DOMINION UNIVERSITY
NORFOLK, VIRGINIA

Technical Report 76-T13

INFRARED BAND ABSORPTANCE CORRELATIONS AND APPLICATIONS TO NONGRAY RADIATION

By

S.N. Tiwari

and

S.V.S. Manian

Progress Report

Prepared for the
National Aeronautics and Space Administration
Langley Research Center
Hampton, Virginia

Under
Research Grant NSG 1282
March - June 1976

June 1976

SCHOOL OF ENGINEERING
OLD DOMINION UNIVERSITY
NORFOLK, VIRGINIA

Technical Report 76-T13

INFRARED BAND ABSORPTANCE CORRELATIONS AND APPLICATIONS TO NONGRAY RADIATION

By

S.N. Tiwari

and

S.V.S. Manian

Progress Report

Prepared for the
National Aeronautics and Space Administration
Langley Research Center
Hampton, Virginia 23665

Under
Research Grant NSG 1282
March - June 1976
Dr. Henry G. Reichle, Technical Monitor
Environmental and Space Sciences Division

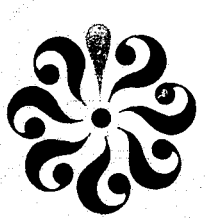

Submitted by the
Old Dominion University Research Foundation
Norfolk, Virginia 23508

June 1976

FOREWORD

This report constitutes a part of the work done on the research project entitled "Determination of Atmospheric Pollutants from Infrared Radiation Measurements." The work was supported by the NASA-Langley Research Center through Grant NSG-1282. The grant was monitored by Dr. Henry G. Reichle.

TABLE OF CONTENTS

LIST OF FIGURES

INFRARED BAND ABSORPTANCE CORRELATIONS AND APPLICATIONS TO NONGRAY RADIATION

by

S. N. Tiwari and S.V.S. Manian

School of Engineering

Old Dominion University

Norfolk, Virginia 23508

SUMMARY

Various molecular band models for infrared radiation are reviewed and continuous correlations for the total absorptance of a wide band are presented. Different band absorptance correlations are employed in two physically realistic problems (radiative transfer in gases with internal heat source and heat transfer in laminar flow of absorbing-emitting gases between parallel plates) to study their influence on final radiative transfer results.

1. INTRODUCTION

The object of this study is to review the molecular band models available in the literature [1-14]* and establish their use for atmospheric applications. Special attention is directed towards obtaining the wide band absorptance relations from the basic formulations of the narrow band models. Several continuous correlations for the total absorptance of a wide band are available in the literature [11-15]. These are employed in two physically realistic radiative transfer analyses to study their effects on the final results of actual radiative transfer process. The first problem considered is the problem of radiative energy transfer between a gas volume and the surrounding walls. The physical concept of this problem can be applied to the radiative transfer analyses of plane-parallel atmosphere with non-uniform heating. The second problem considered is that of a laminar flow of an absorbing-emitting gas between parallel surfaces. Attention is directed, in particular, to carbon monoxide, carbon dioxide, methane, and water vapor.

---

*Numbers in the brackets indicate references.

2. BAND ABSORPTANCE AND CORRELATIONS

The total absorption of a band of overlapping lines strongly depends upon the line intensity, the line half-width, and the spacing between the lines. In a particular band, the absorption coefficient varies very rapidly with the frequency and, therefore, it becomes very difficult and time-consuming task to evaluate the total band absorptance by numerical integration over the actual band contour. Consequently, several approximate band models have been proposed [1-14] which represent absorption from an actual band with reasonable accuracy. The expressions for absorptance by various band models, and several correlations for the total band absorptance are presented in this section. These results are useful in the radiative transfer analyses presented in Sec. III.

The absorption within a narrow spectral interval of a vibration rotation band can quite accurately be represented by the so-called "narrow band models." For a homogeneous path, the total absorptance of a narrow band is given by

$$A = \int_{\Delta\omega} [1-\exp(\kappa_\omega X)]\, d\omega \,, \tag{2.1}$$

where κ_ω is the mass absorption coefficient, $X = \rho_a \ell$ is the mass of the absorbing gas per unit area, ℓ is the length measured along the direction of the path which makes an angle θ with the vertical, and ρ_a is the density of the absorbing gas. The limits of integration in Eq. (2.1) are over the narrow band pass considered.

Four commonly used narrow band models are Elsasser, Statistical, Random Elsasser, and Quasi-Random. The application of a model to a particular case depends upon the nature of the absorbing-emitting molecule. Complete discussions on narrow band models, and expressions for transmittance and integrated

absorptance are available in the literature [1-6,13,14].

The total band absorptance of the so-called "wide band models" is given by

$$A = \int_{-\infty}^{\infty} [1-\exp(-\kappa_\omega X)]\, d(\omega-\omega_o) \ , \tag{2.2}$$

where the limits of integration are over the entire band pass and ω_o is the wave number at the center of the wide band.

In actual radiative transfer analyses, the quantity of frequent interest is the derivative of Eqs.(2.1) and (2.2). With reference to Eq.(2.2), this can be expressed as

$$dA/dX = A'(\kappa_\omega, X) = \int_{-\infty}^{\infty} [\kappa_\omega \exp(-\kappa_\omega X)]\, d(\omega-\omega_o) \ . \tag{2.3a}$$

For multiband gases, Eq. (2.3a) can be written as

$$A' = \sum_{i=1}^{n} A_i'(\kappa_{\omega i}, X) = \sum_{i=1}^{n} \int_{\Delta\omega_i} [\kappa_{\omega i} \exp(-\kappa_{\omega i} X)]\, d(\omega_i-\omega_{oi}) \ , \tag{2.3b}$$

where $\Delta\omega_i$ is the spectral range of the ith wide band and n represents the number of important bands of the absorbing-emitting gas under consideration.

2.1 Exponential Wide Band Absorptance from Narrow Band Models

Detailed discussions on the wide band models are available in the literature [7-15]. The important formulations pertaining only to the exponential wide band models are presented here. The relations for integrated (total) band absorptance for these wide bands are obtained from the absorptance formulations of narrow band models by applying the following relation for the variation of line intensity [10,13-15].

$$S_j/d = (S/A_o) \exp \{[-b_o|\omega-\omega_o|]/A_o\} , \tag{2.4}$$

where S_j is the intensity of the jth spectral line, d is the line spacing, S is the integrated intensity of a wide band, A_o is the band width parameter, and $b_o = 2$ for a symmetrical band and $b_o = 1$ for bands with upper and lower wave number heads at ω_o. The total absorptance of a exponential wide band is obtained from the absorptance of narrow band models by employing the relation

$$\bar{A}(u,\beta) \equiv A(u,\beta)/A_o = \int_{\text{wide band}} [\bar{A}_N (u,\beta)] \, d(\omega-\omega_o) , \tag{2.5}$$

where $u = SX/A_o$ is the nondimensional path length, $\beta = 2\pi\gamma_L/d$ is the line structure parameter, γ_L is the Lorentz line hald-width, and $A_N(u,\beta)$ represents the mean absorptance of a narrow band.

By employing the Elsasser narrow band absorptance relation and Eq.(2.4), the expression for the exponential wide band absorptance is obtained as [13,14]

$$\bar{A}(u,\beta) = \gamma + (1/\pi) \int_o^\pi [\ell n \, \psi + E_1(\psi)] \, dz , \tag{2.6}$$

where $\psi = u \sinh \beta/(\cosh \beta - \cos z)$, $\gamma = 0.5772156$ is the Euler's constant, and $E_1(\psi)$ is the exponential integral of the first order. Analytic solution of Eq.(2.6) can be obtained in a series form as [13]

$$\left.\begin{aligned} A(u,\beta) &= \sum_{n=1}^{\infty} \{-(A)^n [SUM(mn)]/[n(B+1)^n n! \, (n-1)!]\} , \\ \text{where} \quad SUM(mn) &= \sum_{m=o}^{\infty} [(n+m-1)! \, (2m-1)! \, C^m]/[2^m (m!)^2] , \\ A &= -u \tanh \beta, \; B = 1/\cosh \beta , \; C = 2/(1 + \cosh \beta) = 2B/(B+1) . \end{aligned}\right\} \tag{2.7}$$

It can be shown that the series in Eq.(2.7) converges rapidly. When the weak line approximation for the Elsasser model is valid (i.e., β is large), then Eq.(2.6) reduces to [13,14]

$$\bar{A}(u) = \gamma + \ell n\,(u) + E_1(u) \ . \tag{2.8}$$

In the linear and logarithmic limits, Eqs.(2.6) and (2.7) reduce to

$$\left.\begin{aligned} \bar{A} &= u \ , && (u \ll 1 \ , \ \beta > 1) \\ \bar{A} &= \gamma + \ell n(u) \ , && (u \gg 1 \ , \ \infty > 1) \ . \end{aligned}\right\} \tag{2.9}$$

It can be shown that Eq.(2.6) reduces to the correct limiting form in the square-root limit [14].

By employing the uniform statistical narrow band absorptance relation and Eq.(2.4), the expression for the exponential wide band absorptance is obtained as [13,14]

$$\left.\begin{aligned} \bar{A}(u,\beta) &= \int_0^1 \{1-\exp[-\beta\, L(\eta)]\}\, \zeta^{-1}\, d\zeta \ , \\ \text{where} \qquad \eta &= u\zeta/\beta \ , \quad \zeta = \exp[-b_o|\omega-\omega_o|/A_o] \ . \end{aligned}\right\} \tag{2.10}$$

In the limit of large β , this reduces to Eq.(2.8), and the linear and logarithmic limits are given by Eq.(2.9). This also reduces to the correct limiting form in the square-root limit [14].

By employing the general statistical narrow band absorptance relation and Eq.(2.4), a third expression for the exponential wide band absorptance is obtained as [13-15]

$$\left.\begin{aligned}
\bar{A}(u,\beta) &= \int_0^1 \{[1-\exp(-t)]/[\xi^2 + (2\rho_u)^2]^{1/2}\}\, d\xi \\
&\quad + \int_1^1 \{[1-\exp(-\rho t)]/\xi\} d\xi \ , \\
\text{where} \qquad \rho &= [1+(u\zeta/t)] - 1/[1+(u\zeta/t)] \ , \\
\rho_u &= \{(t/u)[1+(t/u)]\}^{-1/2} \ , \\
\xi &= \rho/\rho_u \ , \quad t = \beta/2 = \pi\, \gamma_L/d \ .
\end{aligned}\right\} \qquad (2.11)$$

In the linear and logarithmic limits, this reduces to the expressions given by Eq.(2.9).

A fourth expression for the exponential wide band absorptance is obtained from the narrow random Elsasser model as [13,14]

$$\bar{A}(u,\beta) = \ell n\{[G_2(u,\beta) + u \sinh \beta + \cosh \beta]/(\sinh \beta + \cosh \beta)\} \ , \qquad (2.12)$$

where

$$G_2(u,\beta) = [(u^2 + 1) \sinh^2 \beta + 2u \sinh \beta \cosh \beta]^{1/2} \ .$$

It may easily be shown that Eq.(2.12) satisfies the linear, square-root and logarithmic limits for appropriate u values [14].

The solutions of the four wide band absorptance listed above are termed as the exact solutions. These are illustrated in Fig. 2.1 for three different values of the line structure parameter β. The agreement between the results of various models are found to be within 25%. Since the absorption at small path lengths is a function solely of the total intensity of absorbing lines, the results by all models agree well in this region. At

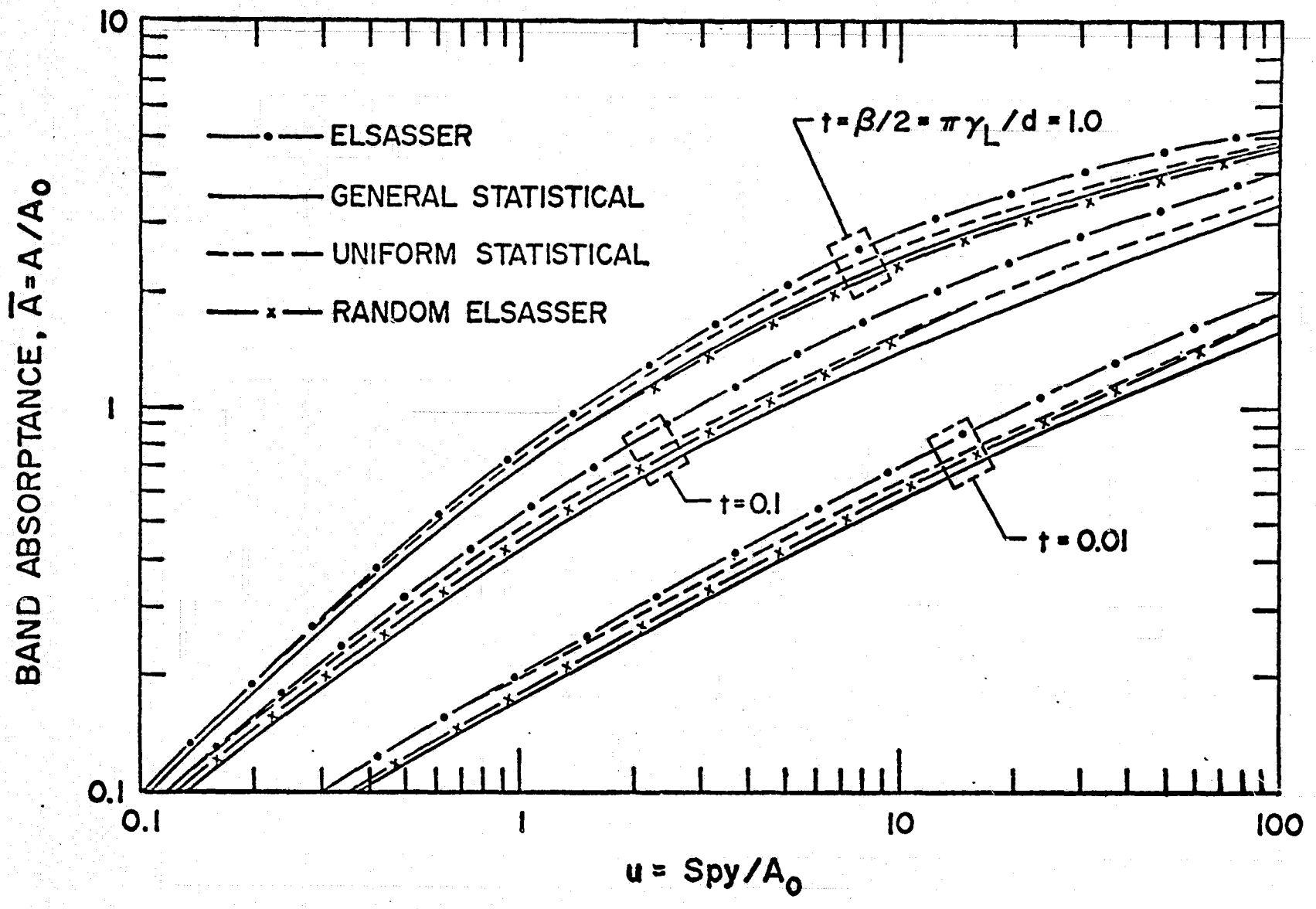

Fig. 2.1 Comparison of absorptance by wide band models.

larger path lengths, however, the Elsasser model predicts higher absorption than the general or uniform statistical model. This is because there is always more overlapping of the spectral lines in the statistical models than in the regular Elsasser band. The main reason for presenting these results here is because various correlations based on these results are employed in actual radiative transfer analyses in Sec. III.

2.2 Band Absorptance Correlations

Several continuous correlations for the total absorptance of a wide band, which are valid over different values of path length and line structure parameter, are available in the literature. These are discussed, in detail, in [11-15] and are presented here in the sequence they become available in the literature. Most of these correlations are developed to satisfy at least some of the limiting conditions (nonoverlapping line, linear, weak line, and strong line approximations, and square-root, large pressure, and large path length limits) for the total band absorptance [12,14]. Some of the correlations even have experimental justifications [8,11]. The results of these correlations are compared in Fig. 2.2 for t = 0.01 and 1. Figure 2.3 shows the errors encountered in using the various correlations as compared with the exact solution obtained by the general statistical model, Eq.(2.11). For comparison of other results, one should refer to [13,14].

(a) Tien and Lowder [11]:

$$\left.\begin{aligned} \bar{A}(u,\beta) &= \ell n(uf(t)\ \{(u+2)/[u+2f(t))]\} +1)\ , \\ \text{where} \qquad f(t) &= 2.94\ [1-\exp(-2.60\ t)]\ ,\quad t = \beta/2\ . \end{aligned}\right\} \tag{2.13}$$

This correlation does not reduce to the correct limiting form in the square-root limit [12], and its use should be made for $\beta \geq 0.1$.

(b) Goody and Belton [16]:

$$\bar{A}(u,\beta) = 2\ \ell n\ \{1 + u/[4 + (\pi u/4t)]^{1/2}\}\ ,\quad \beta = \frac{2t}{\ldots} \tag{2.14}$$

The use of this correlation should be made for relatively small β values [12].

(c) Tien and Ling [17]:

$$\bar{A}(u) = \sinh^{-1}(u) \ . \tag{2.15}$$

This relation is valid only for the limit of large β .

(d) Cess and Tiwari [12-14]:

$$\left.\begin{aligned} \bar{A}(u,\beta) &= 2\ \ell n(1+u/\{2+[u(1+1/\bar{\beta})]^{1/2}\}) \ , \\ \text{where} \qquad \bar{\beta} &= 4t/\pi = 2\beta/\pi \ . \end{aligned}\right\} \tag{2.16}$$

The use of this correlation is justified at relatively high pressures to gases whose spectral behavior can be described by the general statistical model. By slightly modifying Eq.(2.16) another form of the wide band absorptance is obtained as [13,14]

$$\left.\begin{aligned} \bar{A}(u,\beta) &= 2\ \ell n(1+u/\{2+[u(c+\pi/2\beta)]^{1/2}\}) \\ \text{where} \qquad c &= \begin{cases} 0.1 \ , & \beta \leq 1 \ \text{ and all } \ u \ \text{ values} \\ 0.1 \ , & \beta > 1 \ \text{ and } \ u \leq 1 \\ 0.25 \ , & \beta > 1 \ \text{ and } \ u > 1 \end{cases} \end{aligned}\right\} \tag{2.17}$$

Equations (2.16) and (2.17) reduce to all the limiting forms [12]. The results of these correlations are compared with other correlations in Figs. 2.2 and 2.3 .

(e) Edwards and Balakrishnan [10]:

$$\bar{A}(u) = \ell n(u) + E_1(u) + \gamma + \frac{1}{2} - E_3\ (u) \ . \tag{2.18}$$

This correlation is valid for large β and for large values of path lengths (see Figs. 2.2 and 2.3).

(f) Felske and Tien [15]:

$$A(u,\beta) = 2\,E_1(t\rho_u) + E_1(\rho_u/2 - E_1[(\rho_u/2)(1+2t)] + \ell n[(t\rho_u)^2/(1+2t)] + 2\gamma \,. \tag{2.19}$$

This correlation is valid for the entire range of the governing parameters (Fig. 2.2). The comparison of results of this correlation with the exact solution of Eq.(2.11) indicates excellent agreement (Fig. 2.3). This, however, would be expected because the correlation was obtained from Eq. (2.11).

(g) Tiwari and Batki [13,14]. The form of the absorptance given by Eq. (2.8) can be treated as another correlation for the total band absorptance. The use of this correlation is justified at all path lengths for $t = (\beta/2) \geq 1$ (Fig. 2.2).

A comparison of results presented in Figs. 2.1 and 2.2 indicates that Tien and Lowder's correlation follows the general trend of the Elsasser model while Cess and Tiwari's correlation follows the general statistical model. This fact was noted clearly from several comparative results presented in [14]. It was indicated in [14] that results of various correlations could be in error up to 40% when compared with the exact solutions based on different band models. Tien and Lowder's correlation was found to give the least error when compared with the exact solution based on the Elsasser model for t = 0.1, 1, and 10.

From the comparsion of results presented in Figs. 2.2 and 2.3 (and from results of references [13,14]), it may be concluded that the correlation of Felske and Tien provides fairly accurate results for all pressures and path lengths. At relatively high pressures, however, the correlation given by Eq.(2.8) provides a uniformly better approximation for the total band absorptance. While Felske and Tien's correlation is suitable for radiative transfer analyses in gases exhibiting statistical spectral behavior, a better correlation is needed for gases whose spectral characteristics warrant use of the Elsasser model. One such relation is given by Eq.(2.7) which is the series form solution of the Elsasser total band absorptance.

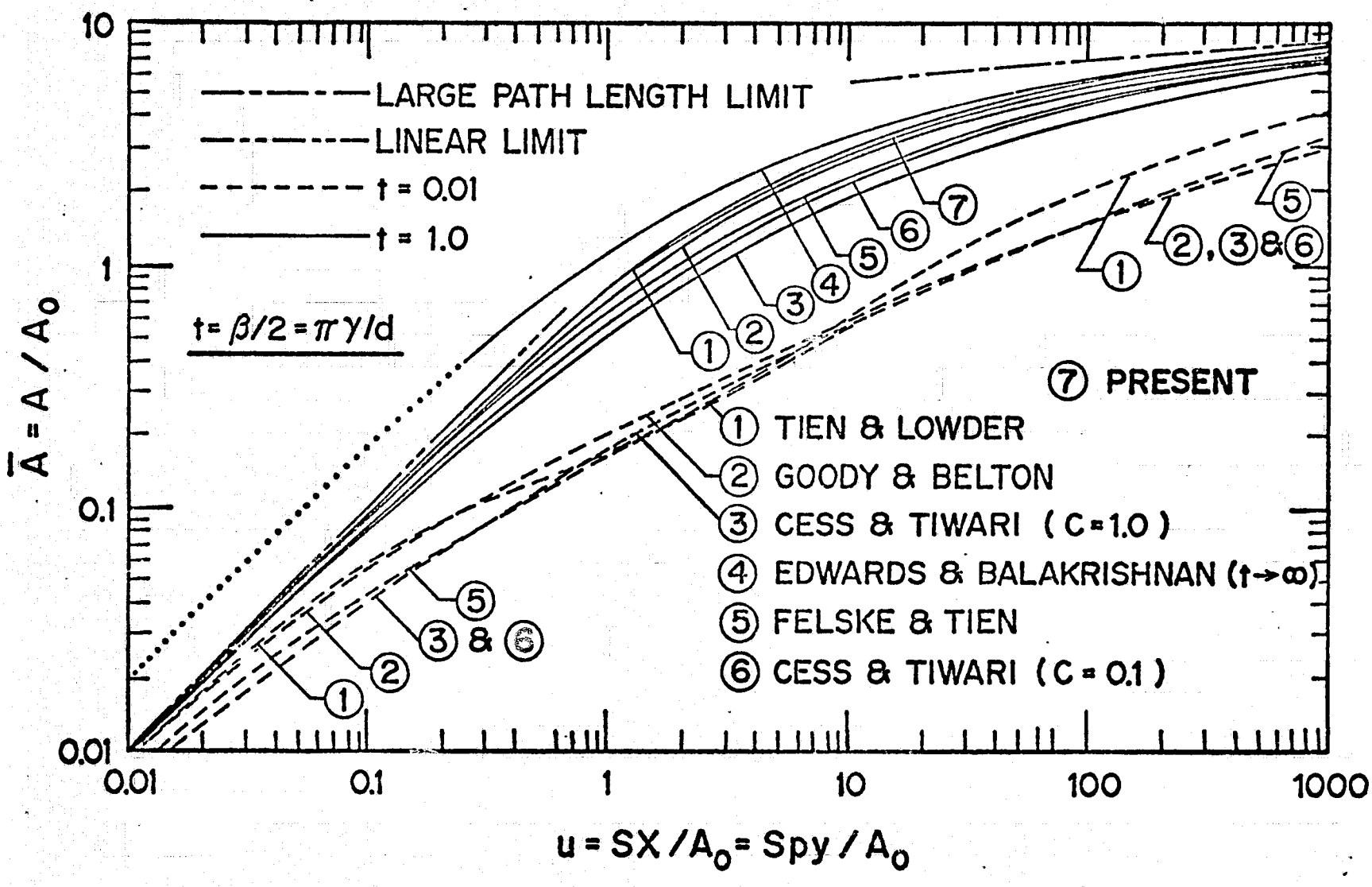

Fig. 2.2 Comparison of results of band absorptance correlations for t = 0.01 and 0.1.

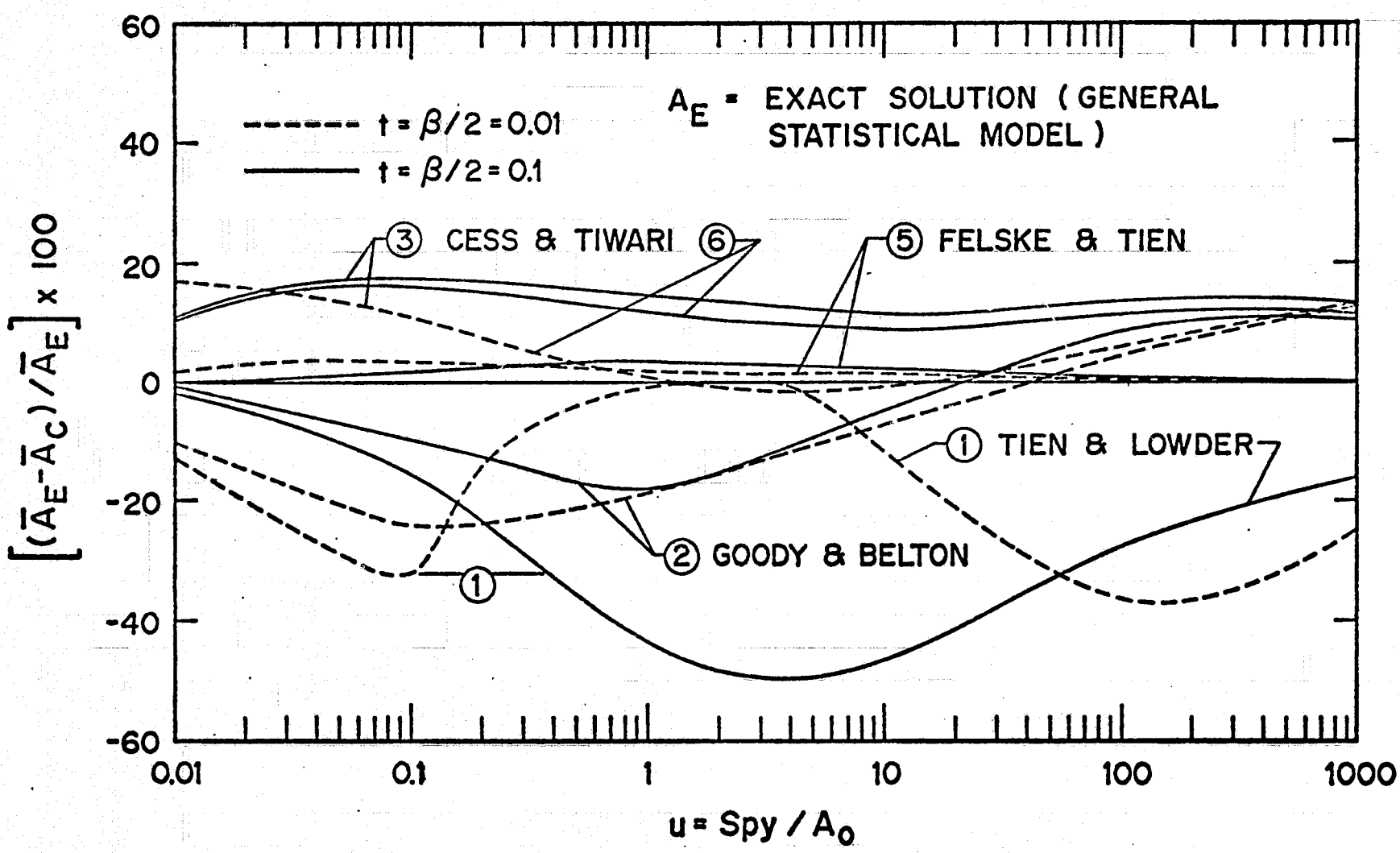

Fig. 2.3 Errors in the band absorptance correlations when compared with the exact solution (General Statistical Model) for t = 0.01 and 0.1.

3. RADIATIVE TRANSFER ANALYSES

The band absorptance correlations discussed in the previous section are employed in this section to two illustrative radiative transfer problems. The physical model and coordinate systems for both problems are shown in Fig. 3.1 .

The expression for the total radiative flux may, in general, be given by [12,18]

$$q_R = \int_o^\infty q_{R\omega}\, d\omega = e_1 - e_2$$

$$+ \frac{3}{2} \int_o^y [e_{\omega_o}(z) - e_{\omega_o}(T_1)] \int_{\Delta\omega} \kappa_\omega \exp[-\tfrac{3}{2}\kappa_\omega(y-z)]\, d\omega\, dz$$

$$- \frac{3}{2} \int_y^L [e_{\omega_o}(z) - e_{\omega_o}(T_2)] \int_{\Delta\omega} \kappa_\omega \exp[-\tfrac{3}{2}\kappa_\omega (z-y)]\, d\omega\, dz \ , \qquad (3.1)$$

where $e = \sigma T^4$, with σ denoting the Stefan-Boltzmann constant, and $\Delta\omega$ indicates integration over the single band. The derivation of Eq.(3.1) assumes the existence of a local thermodynamic equilibrium and employes the exponential kernal approximation. The Planck function, $e_\omega(T)$, is considered a slowly varying function of wave number over the narrow band and its value is evaluated at the band center. The primary motivation for employing the exponential kernal approximation is that it allows the kernal function in Eq.(3.1) to be expressed in terms of the derivative of the total band absorptance which is given by Eq.(2.3).

A combination of Eqs.(2.3) and (3.1) results in

$$q_R(\xi) = e_1 - e_2 + \frac{3}{2} A_o u_o \{ \int_o^\xi [e_{\omega_o}(\xi') - e_{\omega_o}(T_1)] \bar{A}'[\tfrac{3}{2} u_o(\xi-\xi')]\, d\xi'$$

$$- \int_\xi^1 [e_{\omega_o}(\xi') - e_{\omega_o}(T_2)] \bar{A}'[\tfrac{3}{2} u_o(\xi'-\xi)]\, d\xi' \} \ , \qquad (3.2)$$

where $\xi = y/L$, $u_o = S(T_1)\ p\ L/A_o(T_1)$, $\bar{A}(u,\beta) = A(u,\beta)/A_o$.

In this equation, $\bar{A}'(u)$ denotes the derivative of $\bar{A}(u)$ with respect to u and u_o represents the nondimensional pressure path length. Equation (3.2) possesses two limiting forms (optically thin and large path length limits) which are discussed in detail in [12,19,20]. It should be pointed out here that while the large path length limit may depend upon a particular band model employed in the radiative flux equation, the optically thin limit is completely independent of the band model.

In order to study the effect of different band absorptance correlations on the final results of actual radiative transfer processes, two illustrative cases (extensively studied in the literature) are treated here. The first is the problem of radiative energy transfer between a gas volume (where there is a uniform heat source) and the surrounding walls. The physical concept of this problem can be applied to the radiative transfer analyses of plane-parallel atmosphere with non-uniform heating. The second problem considered is the problem of liminar flow of absorbing-emitting gases between parallel surfaces. This represents a realistic situation of convective-radiative energy transfer in the atmosphere and in other engineering problems. For mathematical simplicity, the bounding surfaces for both problems are considered to be black.

3.1 Radiative Transfer in Gases with Internal Heat Source

The physical model and the coordinate system for this case is shown in Fig. 3.1a . The two parallel black walls are considered to be at the same constant temperature T_1 . The gas is assumed to have a uniform heat source (or sink) of strength Q per unit volume. The radiative transfer is the

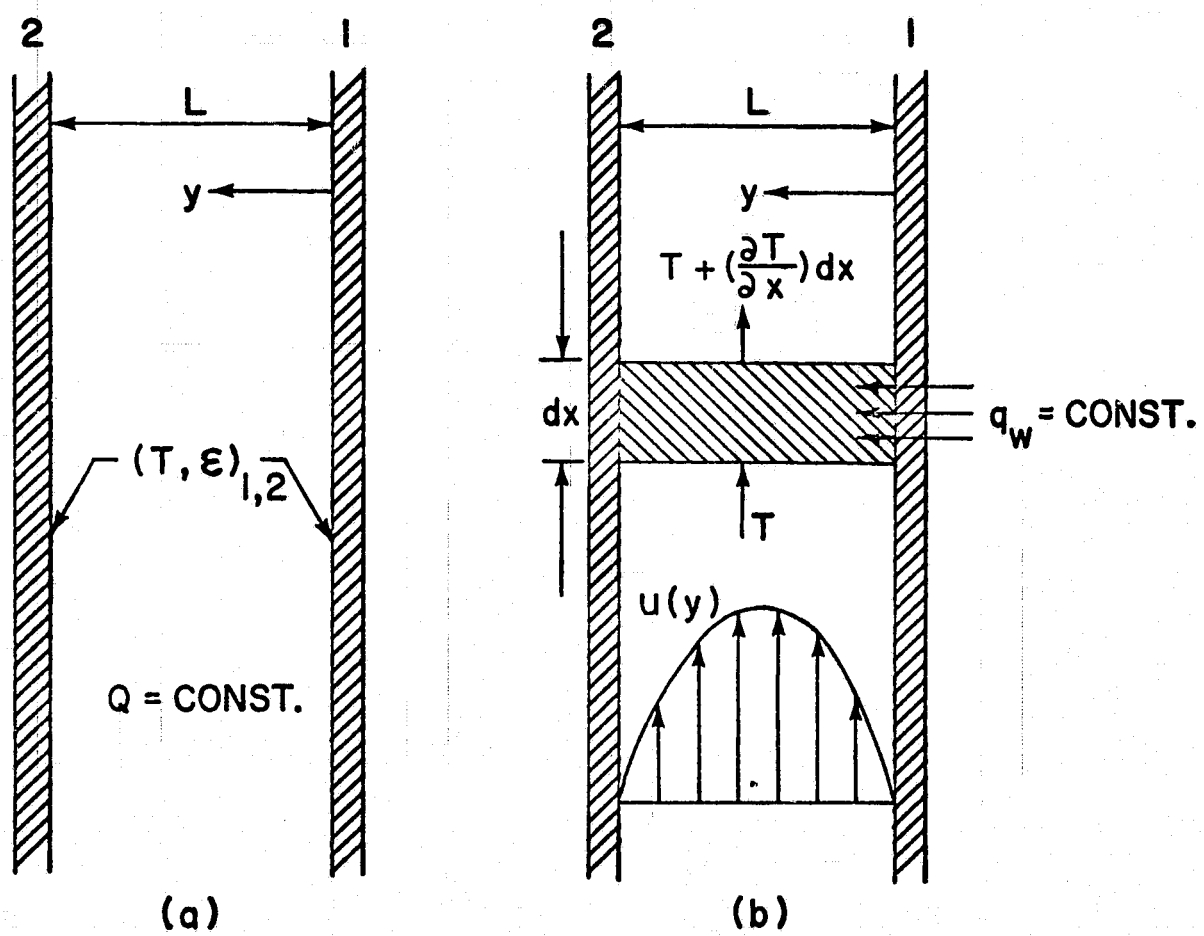

Fig. 3.1 Physical model and coordinate system.

sole mechanism of energy transfer within the gas. The local temperature distribution is thus a consequence of the uniform heat source adding energy to the gas which in turn is transferred through the gas to the bounding surfaces by radiative transfer.

For this special case the conservation of energy yields

$$dq_R/dy = Q \tag{3.3}$$

Since the problem is symmetric, an integration of Eq.(3.3) gives $q_R = (1/2)\ Q\ L\ (2\xi - 1)$ and after combining this with Eq.(3.2) results in

$$\left.\begin{aligned} \xi - \frac{1}{2} = \frac{3}{2}\Big\{ & \int_0^{\xi} \phi(\xi')\bar{A}'\left[\frac{3}{2}\,u_o(\xi-\xi')\right] d\xi' \\ & - \int_{\xi}^{1} \phi(\xi')\ \bar{A}'\left[\frac{3}{2}\,u_o(\xi'-\xi)\right] d\xi'\Big\}\ , \end{aligned}\right\} \tag{3.4}$$

where $\phi(\xi) = [e_{\omega_o}(T) - e_{\omega_o}(T_1)]/(Q/PS(T_1))$.

In this equation $\phi(\xi)$ represents the temperature profile within the gas in terms of the Planck function. The equation is written for a single band gas but it can easily be extended to the case involving multi-band gases [12].

In the optically thin limit (i.e., for $u_o \ll 1$) , $\bar{A}(u) = u$, and $\bar{A}'(u) = 1$ such that Eq.(3.4) yields the result [12,20]

$$\phi(\xi) = 1/3\ . \tag{3.5}$$

For most band models, the band absorptance in the large path length limit (i.e., for $u_o \gg 1$) is given by the relation $\bar{A}(u) = \ell n\ (u)$ such that $\bar{A}'(u) = 1/u$. In this limit, therefore, Eq.(3.4) reduces to [12,19]

$$\xi - \frac{1}{2} = \int_0^1 \phi(\xi')\ d\xi'/(\xi-\xi')\ , \tag{3.6}$$

for which the solution is found to be

$$\phi(\xi) = (1/\pi)[\xi(1 - \xi)]^{1/2} . \tag{3.7}$$

As discussed in [12,19], Eq.(3.7) yields the result that the gas temperature at a surface is equal to the surface temperature. This absence of a temperature slip is characteristic of optically thick radiation.

The first information needed for numerical solution of Eq.(3.4) is the derivative of the band absorptance correlations employed in the analysis. Numerical solutions of (3.4) are obtained by using the method of undetermined parameters. In this method a polynomial solution for ϕ is assumed, and the constants are evaluated by satisfying the integral equations at equally spaced locations. If a quadratic solution for ϕ is assumed then $\phi(\xi) = a_o + a_1 \xi + a_2 \xi^2$, and by using the symmetry condition $\phi'(\xi=1/2) = 0$, one obtains

$$\phi(\xi) = a_o + a_1(\xi - \xi^2) . \tag{3.8}$$

The constants a_o and a_1 are evaluated by satisfying Eq.(3.4) at $\xi = 0$ and $1/4$. If quartic solution for ϕ is assumed then by using the symmetry conditions one obtains

$$\phi(\xi) = a_1 - a_2(\xi - \xi^2) - a_3(\tfrac{1}{2} \xi - \xi^3 + \tfrac{1}{2} \xi^4) . \tag{3.9}$$

The constants a_1, a_2, and a_3 are obtained by satisfying Eq.(3.4) at $\xi = 0$, $1/6$, and $1/3$. The choice of locations for satisfying the integral equation to obtain the constants is consistent with the symmetry conditions.

By employing the various band absorptance correlations discussed in the previous section, numerical solutions of Eq.(3.4) were obtained for different values of the line structure parameter $t = \beta/2$. The results are illustrated in Figs. 3.2 - 3.4 along with the limiting solutions. It should be

pointed out here that these results apply to any situation for which radiative transfer within the gas is the result of a single band.

It is obvious from Figs. 3.2-3.4 that the band absorptance results of all the correlations approach the optically thin limit for small u_o , the influence of the line structure parameter is maximum for intermediate values of u_o , and in the large path length limit the solutions become independent of β . The one exception to this is that the results of Goody and Belton's correlation do not approach the correct logarithmic limit for large β . The reasons for this are discussed in [12,14] where it was pointed out that the use of the Goody and Belton's correlation should be restricted to relatively small values of β .

For a particular value of β , the results of different correlations approach the linear and logarithmic limits for different u_o values. For $\beta = 0.02$, for example, the results of all correlations (except Tien and Lowder's) almost are identical for $u_o \geq 1$. This corresponds to the range of the square-root limit where three separate conditions ($\beta \ll 1$, $u/\beta \gg 1$, and $\beta \ll 1$) must be satisfied [12,14]. The square-root limit is not satisfied by the Tien and Lowder's correlation. Although the linear limit is independent of any spectral model, it is approached by different correlations for different u_o values.

Maximum differences between the results of various correlations occur for the intermediate values of u_o ($0.1 < u_o < 10$) and for $0.1 < \beta < 1$. For large β values (i.e., for high pressures), the line structure of a gas is smeared out and differences between the results of various correlations become small (see Fig. 3.4). This situation corresponds to the weak line approximation [14], and some consideration of this usually is given in developing a particular correlation.

In general (and for the intermediate path lengths in particular), the temperature difference between the centerline of the physical system and the wall is found to be lowest for the Tien and Lowder's correlation and highest for the Cess and Tiwari's correlations. For the most part, the results of other correlations fall between these two extreme values. The physical reasoning behind this is consistent with the results of the total band absorptance illustrated in Fig. 2.2. If the absorption by a gas is high, then, to maintain the local thermodynamic equilibrium, the emission by the gas will be higher. This will result in high radiative energy transfer from the gas and consequently will lower the center line temperature. The trend exhibited by the results of Fig. 2.2 and Figs. (3.2 and 3.3) is, therefore, mutually consistent. Thus, the difference in the centerline temperatures, as obtained by using the different correlations, are of the same order as the difference in the band absorptance results of various correlations.

As mentioned in Sec. 2 (see Fig. 2.1), the Elsasser theory always predicts higher absorption than the general statistical model. From this and the results of Figs. 3.2 - 3.4, it may be concluded that for $\beta > 0.02$, use of the Tien and Lowder's correlation is justified for gases whose spectral behavior can be described by the regular Elsasser model. On the other hand, use of the Cess and Tiwari's correlation could be made to gases with bands of highly overlapping lines. Since, in a vibration-rotation band, the lines are distributed neither regularly nor randomly, care should be taken in applying a particular correlation for a specific case.

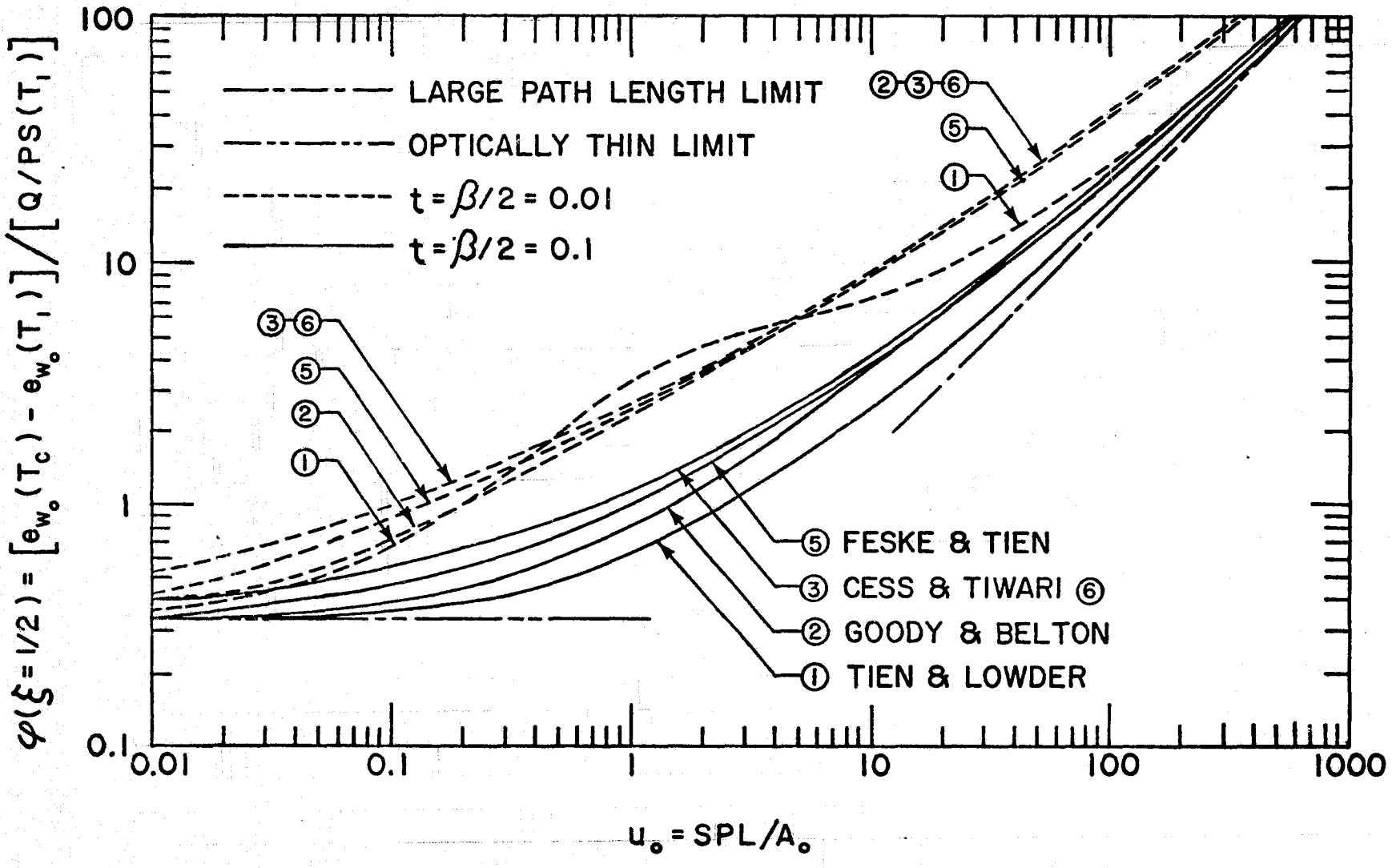

Fig. 3.2 Comparison of results for a single band gas as obtained by using the various band absorptance correlations.

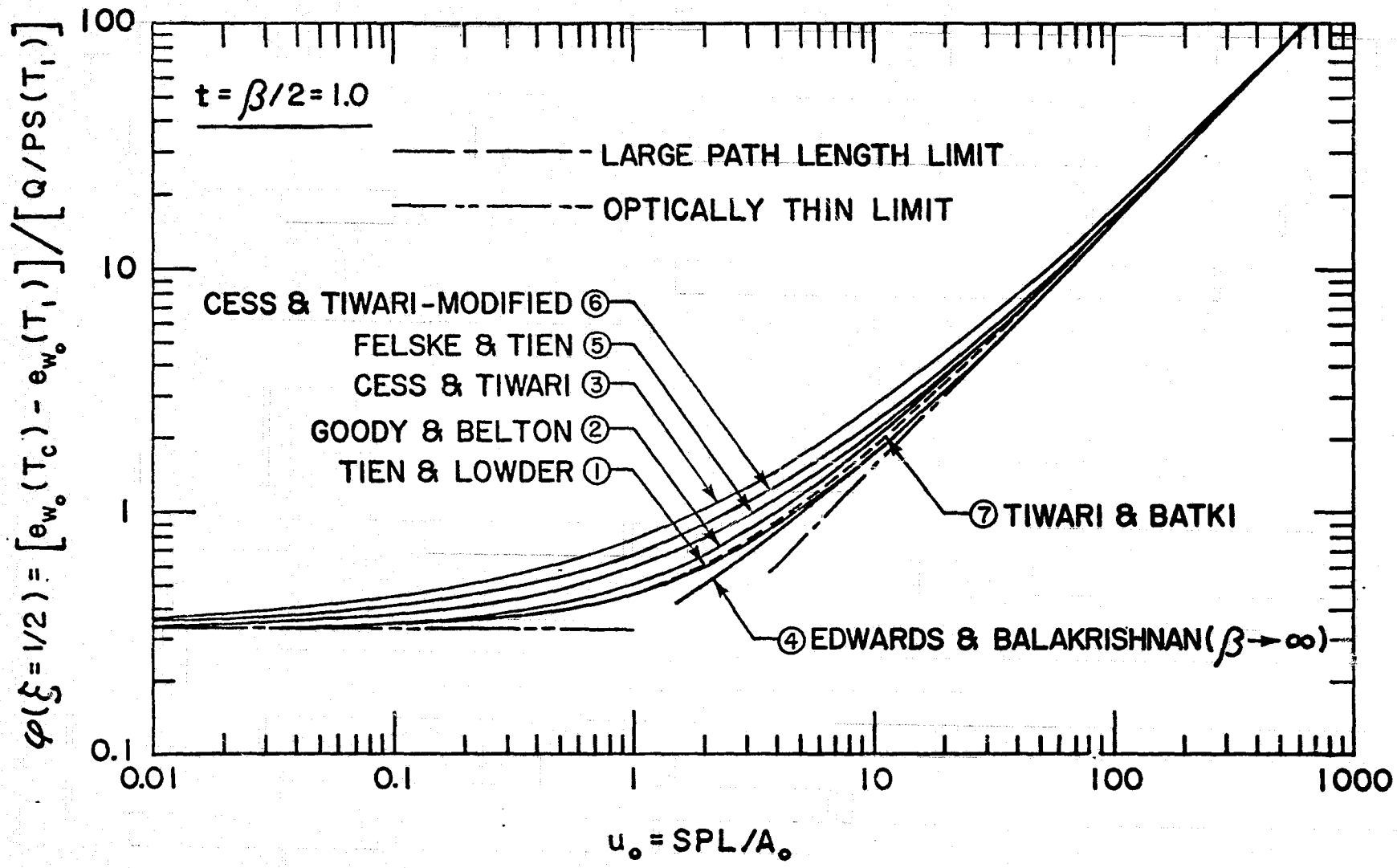

Fig. 3.3 Comparison of results for a single band gas obtained by using the various band absorptance correlations for $t = 1$.

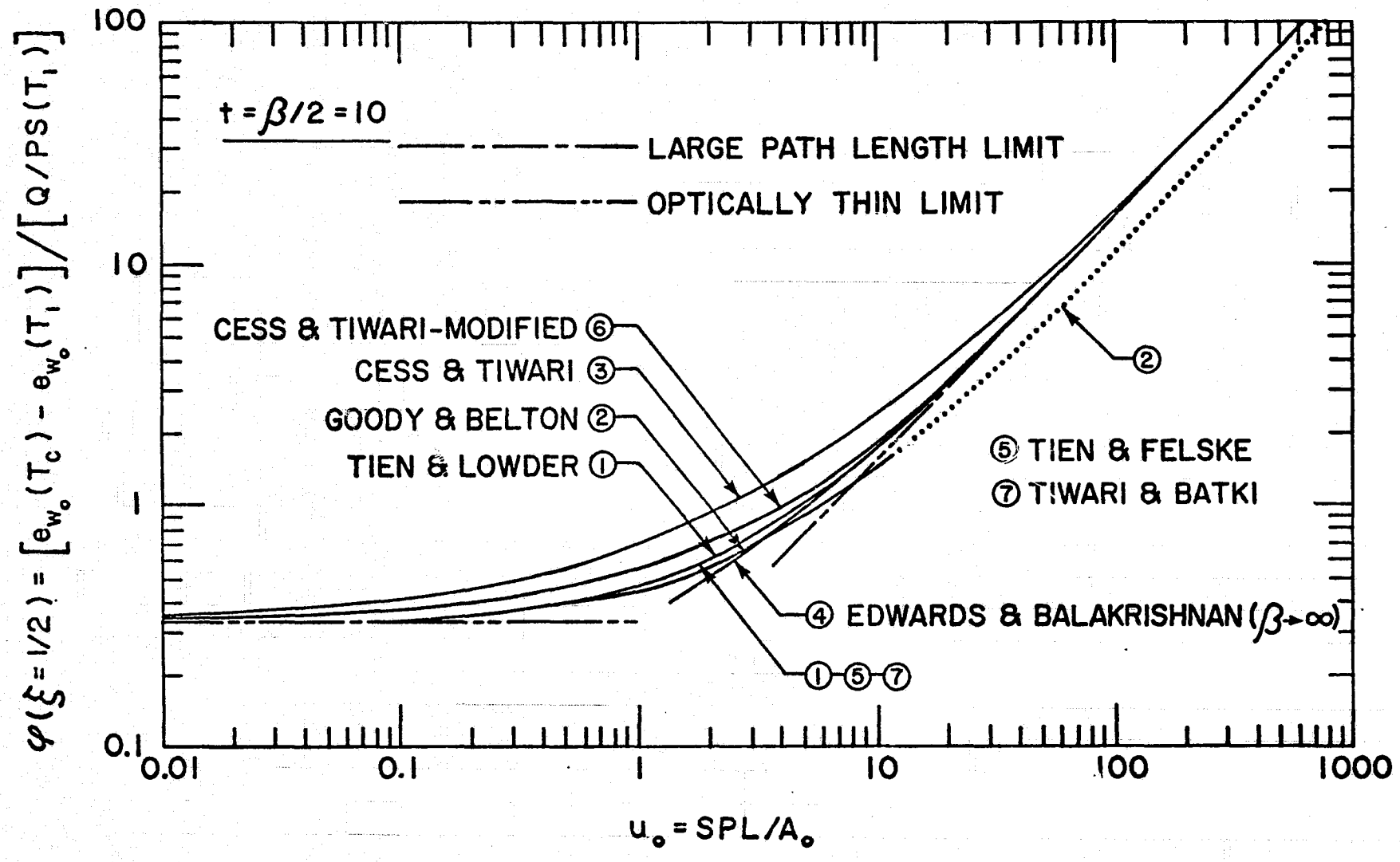

Fig. 3.4 Comparison of results for a single band gas obtained by using the various band absorptance correlations for t = 10.

3.2 Heat Transfer in Laminar Flow of Abosrbing-Emitting Gases Between Parallel Plates

The second problem considered is the problem of heat transfer in laminar, incompressible, constant properties, fully developed flow of absorbing-emitting gases between parallel plates. The physical model and coordinate system for this case is shown in Fig. 3.1b . The conditions of uniform surface heat flux for each plate is assumed such that the temperature of the plates, T_1 , varies in the axial direction. Fully developed heat transfer is considered, and axial conduction and radiation is assumed to be negligible as compared with the normal components. Consistent with the constant properties flow, the absorption coefficient is taken to be independent of temperature and radiation can be linearized. Extensive treatment of this problem is available in the literature [8,12,21-27]. The sole motivation for studying the problem here is to investigate the influence of different band absorptance correlations on the radiative transfer capability of a gas in a more realistic situation.

Within the confines of foregoing assumptions, the energy equation for the present problem can be written as

$$v_x \frac{\partial T}{\partial x} = \alpha \frac{\partial^2 T}{\partial y^2} - \frac{1}{\rho c_p} (\partial q_R / \partial y) \ , \tag{3.10}$$

where the parabolic velocity profile is described by the equation

$$v_x = 6 \ v_m [(y/L) - (y/L)^2] \ . \tag{3.11}$$

The mean velocity v_m is given by the expression

$$v_m = \frac{1}{A_c} \int_{A_c} v_x \, dA_c \ , \tag{3.12}$$

where A_c is the cross-sectional area normal to the direction of flow.

For a uniform wall heat flux and fully developed heat transfer $\partial T/\partial x$ is a constant and is given by the expression

$$\frac{\partial T}{\partial x} = 2 \ \alpha \ q_w / (v_m \ L \ \lambda) \ , \tag{3.13}$$

where λ is the thermal conductivity of the gas.

A combination of Eqs.(3.10) through (3.13) results in

$$12(\xi-\xi^2) = \frac{d^2\theta}{d\xi^2} - \frac{1}{q_w}\frac{dq_R}{d\xi} , \qquad (3.14)$$

where

$$\xi = y/L , \quad \theta = (T-T_1)/(q_w L/\lambda) .$$

Upon integrating this equation once, and by noting that $d\theta/d\xi = 0$ and $q_R = 0$ at $\xi = 1/2$, one finds

$$\frac{d\theta}{d\xi} - 2(3\xi^2 - 2\xi^3) + 1 = q_R/q_w . \qquad (3.15)$$

By combining Eqs.(3.2) and (3.15) the governing integro-differential equation for linearized radiation in multi-band gases can be written as [12]

$$\frac{d\theta}{d\xi} - 2(3\xi^2 - 2\xi^3) + 1 = \frac{3}{2}\frac{L}{\lambda}\sum_{i=1}^{n} H_i u_{oi} \left\{ \int_o^{\xi} \theta(\xi') \bar{A}_i' [\tfrac{3}{2} u_{oi}(\xi-\xi')] d\xi' - \int_{\xi}^{1} \theta(\xi') \bar{A}_i' [\tfrac{3}{2} u_{oi}(\xi'-\xi)] d\xi' \right\} , \qquad (3.16)$$

where

$$\bar{A}_i = A_i/A_{oi} , \quad u_{oi} = S_i(T_1)\, pL/A_{oi}(T_1)$$

$$H_i = A_{oi}(de_{\omega i}/dT)_{T_1} , \quad H = \sum_{i=1}^{n} H_i .$$

In this equation $S_i(T_1)$ is the band intensity and $A_{oi}(T_1)$ is the band width parameter for the ith band. The equation describes the temperature profile within the gas for which the boundary condition can be written as $\theta(0) = 0$.

For flow problems, the quantity of primary interest is the bulk temperature of the gas, which is defined as

$$T_b = \frac{1}{v_m A_c} \int_{A_c} T\, v_x\, dA_c = \frac{1}{v_m L} \int_o^L T\, v_x\, dy \ . \qquad (3.17)$$

By employing Eqs.(3.11) and (3.12) and the nondimensional quantities defined earlier, the bulk temperature can be expressed in a dimensionless form as

$$\theta_b = (T_b - T_1)/(q_w\, L/\lambda) = 6 \int_o^1 \theta(\xi)\, (\xi - \xi^2)\, d\xi \ . \qquad (3.18)$$

The heat transfer q_w is given by the expression, $q_w = h_c(T_1 - T_b)$, where h_c is the convective heat transfer coefficient (btu/hr-sq ft-°F). In general, the heat transfer results are expressed in terms of the Nusselt number Nu, a dimensionless quantity defined as, $Nu = h_c\, D_h/\lambda$. Here, D_h represents the hydraulic diameter, and for parallel plate geometry it equals twice the plates separation, i.e., $D_h = 2L$. Upon eliminating the convective heat transfer coefficient, h_c, from the expressions for q_w and Nu, a relation between the Nusselt number and the bulk temperature is obtained as

$$Nu = 2L\, q_w/\lambda(T_1 - T_b) = -2/\theta_b \ . \qquad (3.19)$$

The general solution of Eq.(3.16) is obtained by numerical procedures. Before discussing the methods of obtaining these solutions, it would be convenient to discuss the limiting forms of the general equation.

For the case of negligible radiation, the divergence of radiative flux is taken to be zero and Eq.(3.14) yields

$$-\theta(\xi) = \xi - 2\xi^3 + \xi^4 \ . \qquad (3.20)$$

By substituting this into Eq.(3.18), the bulk temperature for this case of no radiation is obtained as

$$\theta_b = -\ 17/70 \ . \qquad (3.21)$$

In the optically thin limit Eq.(3.16) reduces to

$$\frac{d\theta}{d\xi} - 2(3\xi^2 - 2\xi^3 + 1) = + \frac{3}{2}\frac{L}{\lambda}\sum_{i=1}^{n} H_i\, u_{oi}\left\{\int_o^{\xi} \theta(\xi')\, d\xi' - \int_{\xi}^{1} \theta(\xi')\, d\xi'\right\} . \tag{3.22}$$

After differentiating once, Eq.(3.22) can be expressed in the following form

$$\frac{d^2\theta}{d\xi^2} - 3\, N\, \theta(\xi) = 12(\xi - \xi^2) , \tag{3.23}$$

for which the boundary conditions are $\theta(0) = 0$, and $\theta'(1/2) = 0$. The quantity N in this equation is referred to as the optically thin radiation-conduction interaction parameter and is given by the relation

$$N = (p\, L^2/\lambda) \sum_{i=1}^{n} S_i(T_1)\, (de_{\omega i}/dT)_{T_1} . \tag{3.24}$$

Equation (3.23) possesses an elementary solution, and the result expressed in terms of the bulk temperature is found to be

$$\left.\begin{aligned} \theta_b &= [1/(3N)^3]\{(576/\sqrt{3N})(NEXP) - 21.6\, N^2 + 72\, N - 288\} , \\ \text{where} \quad NEXP &= [1 - \exp(-\sqrt{3N})]/[1 + \exp(-\sqrt{3N})] . \end{aligned}\right\} \tag{3.25}$$

The results of this equation (θ_b versus N) are illustrated in Fig. 3.5 along with other limiting solutions.

In the large path length limit the band absorptance for each band of importance is given by the relation $\bar{A}_i(u_i) = n(u_i)$ such that $\bar{A}'_i(u_i) = 1/u_i$. Upon substituting this in Eq.(3.16) there is obtained

$$\left.\begin{aligned} \frac{d\theta}{d\xi} - 2(3\xi^2 - 2\xi^3) &= M \int_o^1 \theta(\xi')\, d\xi'/(\xi - \xi') \\ \text{where} \quad M = HL/\lambda &= (L/\lambda)\sum_{i=1}^{n} H_i = (L/\lambda)\sum_{i=1}^{n} A_{oi}(de_{\omega i}/dT)_{T_1} . \end{aligned}\right\} \tag{3.26}$$

The dimensionless parameter M constitutes the radiation-conduction interaction parameter for the large path length limit. Equation (3.26) does not appear to possess a closed form solution. A numerical solution has thus been obtained, and the results for bulk temperature (θ_b versus M) are illustrated in Fig. 3.5 .

Numerical solutions of Eqs.(3.16) and (3.26) are obtained by the method of undetermined parameters. For this case, a polynomial solution for $\theta(\xi)$ is assumed as

$$\theta(\xi) = a_o + a_1\xi + a_2\,\xi^2 + a_3\,\xi^3 + a_4\,\xi^4 \ . \tag{3.27}$$

After employing the conditions $\theta(0) = 0$, $\theta'(1/2) = 0$, and $\theta'(1) = -\theta'(0)$, Eq.(3.27) becomes

$$\theta(\xi) = a_1(\xi - 2\xi^3 + \xi^4) + a_2(\xi^2 - 2\xi^3 + \xi^4) \ . \tag{3.28}$$

The constants a_1 and a_2 are obtained by satisfying the governing integro-differential equation at two locations $\xi = 0$ and $\xi = 1/4$.

A combination of Eqs.(3.18) and (3.28) results in

$$\theta_b = \frac{1}{70}\,(17a_1 + 3a_2) \ . \tag{3.29}$$

Thus, with a_1 and a_2 known, the bulk temperature (or Nusselt number) is obtained from Eq.(3.29).

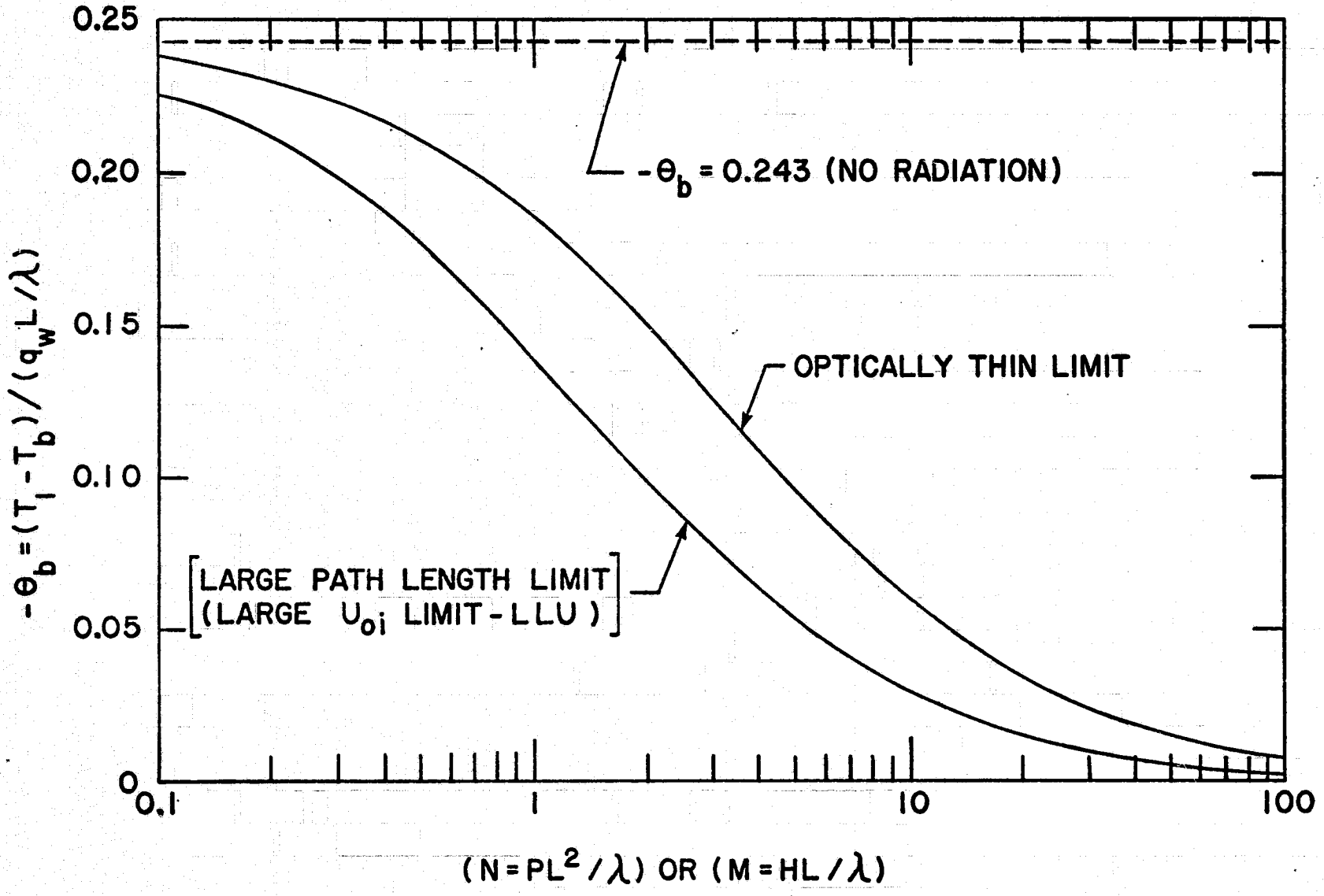

Fig. 3.5 Limiting solutions of the flow problem. The abscissa for optically thin limit is N and for large path length limit is M.

A complete discussion (and physical interpretations) of the various parameters entering into the present problem is given in [12,22,23]. Numerical solutions of Eq. (3.16) were obtained in terms of the bulk temperature (see Eq. (3.29)), and these are presented here in terms of the dimensional quantities L and P. Specific results were obtained for CO (fundamental + 1st overtone bands), CO_2 (15μ, 4.3μ, and 2.7μ bands), H_2O (rotational, 6.3μ, 2.7μ, 1.87μ and 1.38μ bands), and CH_4 (7.6μ and 3.3μ bands) for which spectral information were obtained from [8,11,23].

For CO, CO_2, H_2O, and CH_4, the results obtained by employing the Tien and Lowder's correlation for band absorptance are illustrated in Figs. 3.6 through 3.10. The limiting value of $\theta_b = -0.243$ corresponds to negligible radiation, and the effect of radiation increases with increasing plate spacing. As would be expected, radiative transfer is more pronounced for higher pressures and wall temperatures. Also shown in Figs. 3.6 - 3.9 are the limiting solutions for large u_o (LLU). It is seen that, for a given wall temperature, the large u_o limit can be obtained either by going to large values of L or to high pressures. These results also indicate that, for a particular wall temperature, the large u_o limit for CO_2 is achieved at a relatively lower pressure than for other gases. As a matter of fact, for most practical purposes involving CO_2 at room temperature, the results for one atmosphere can be regarded as the results for the large u_o limit. A comparison of the results for the four gases is shown in Fig. 3.10 for a pressure of one atmosphere and a wall temperature of 1,000 °K. As discussed in [12,19,20], the relative order of the four curves, for small values of L is characteristic of the interaction parameter for optically thin radiation, and for large L is is characteristic of the interaction parameter for the large u_o limit.

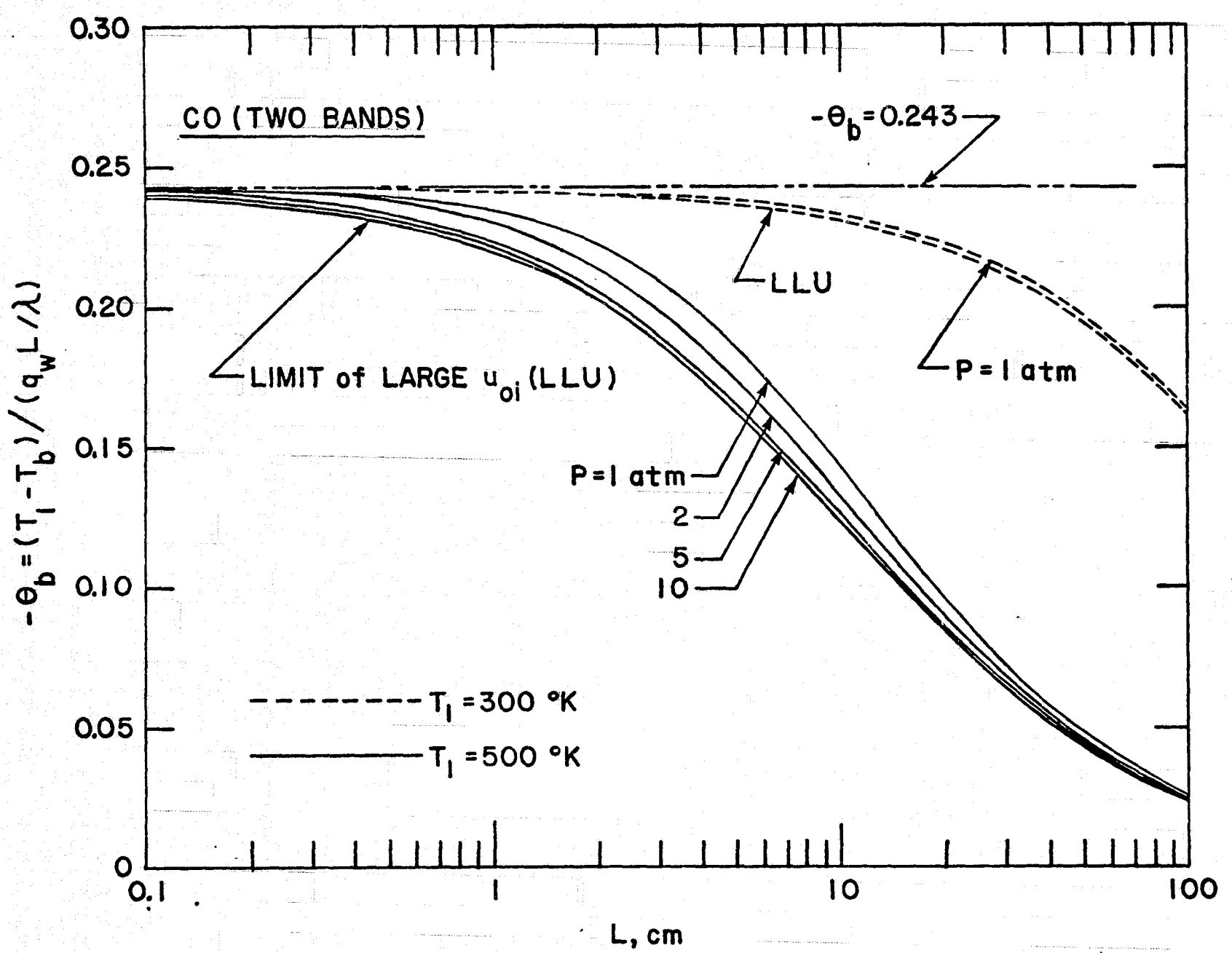

Fig. 3.6a Results for CO obtained by using the Tien and Lowder's correlation.

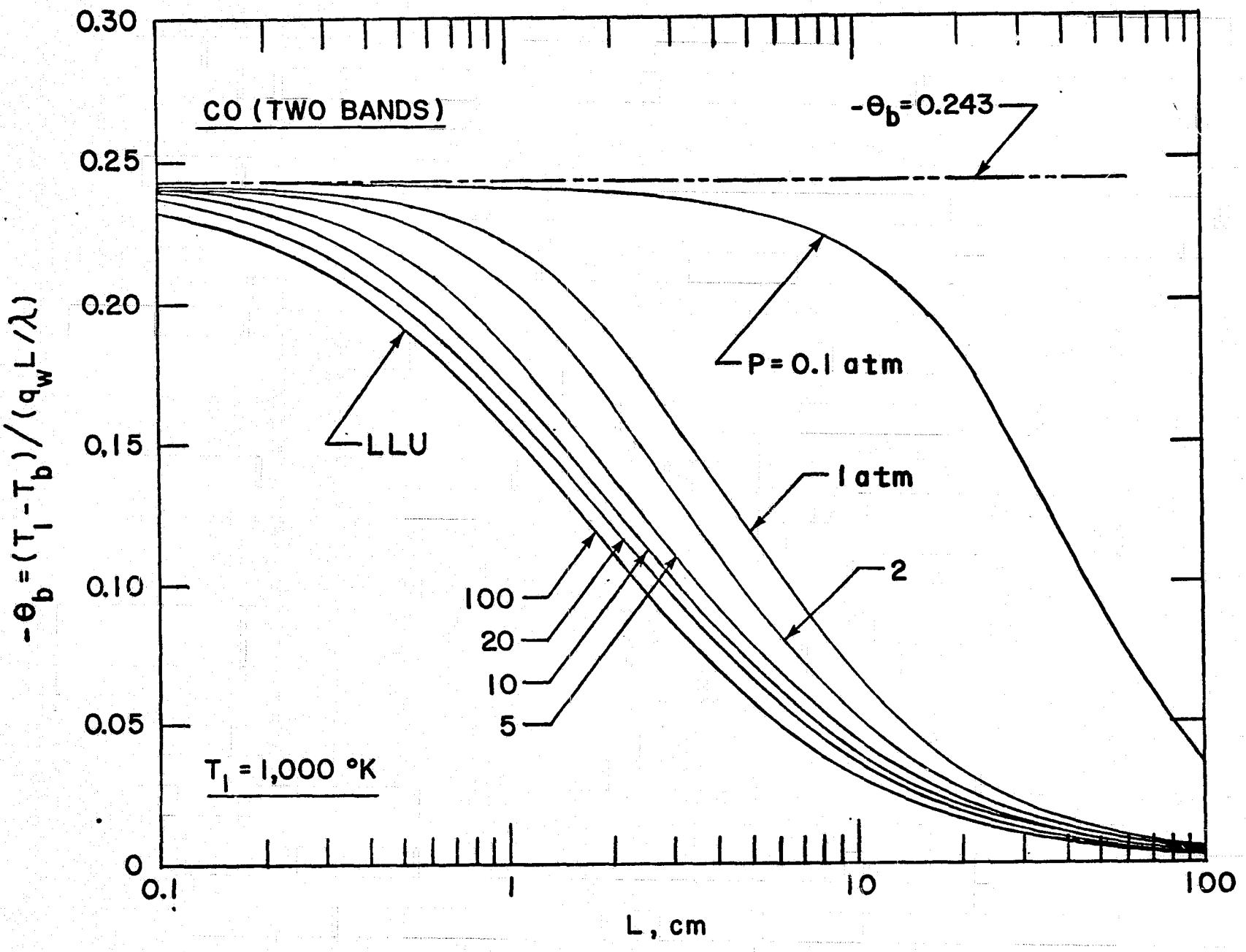

Fig. 3.6b Results for CO obtained by using the Tien and Lowder's correlation.

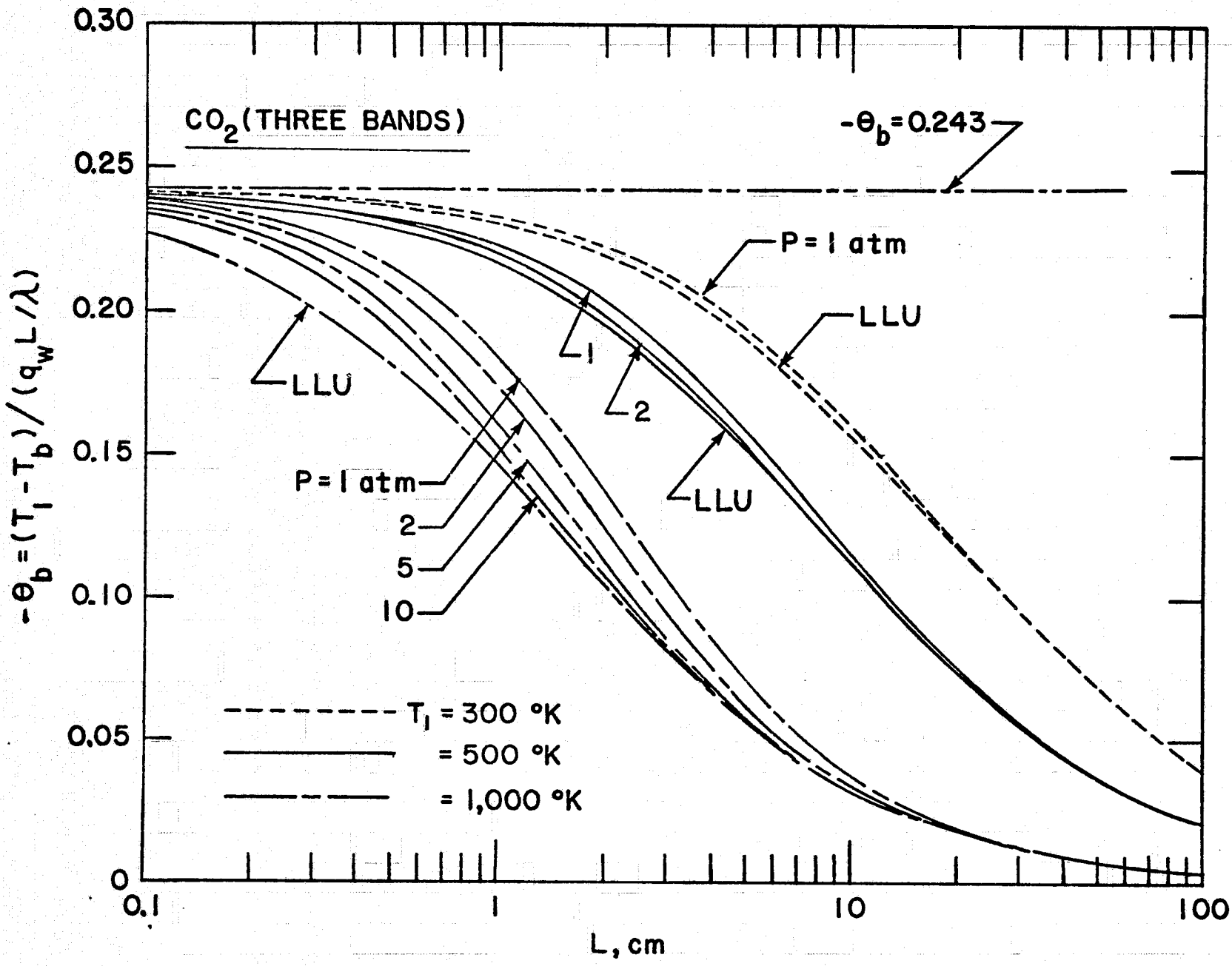

Fig. 3.7 Results for CO_2 obtained by using the Tien and Lowder's correlation.

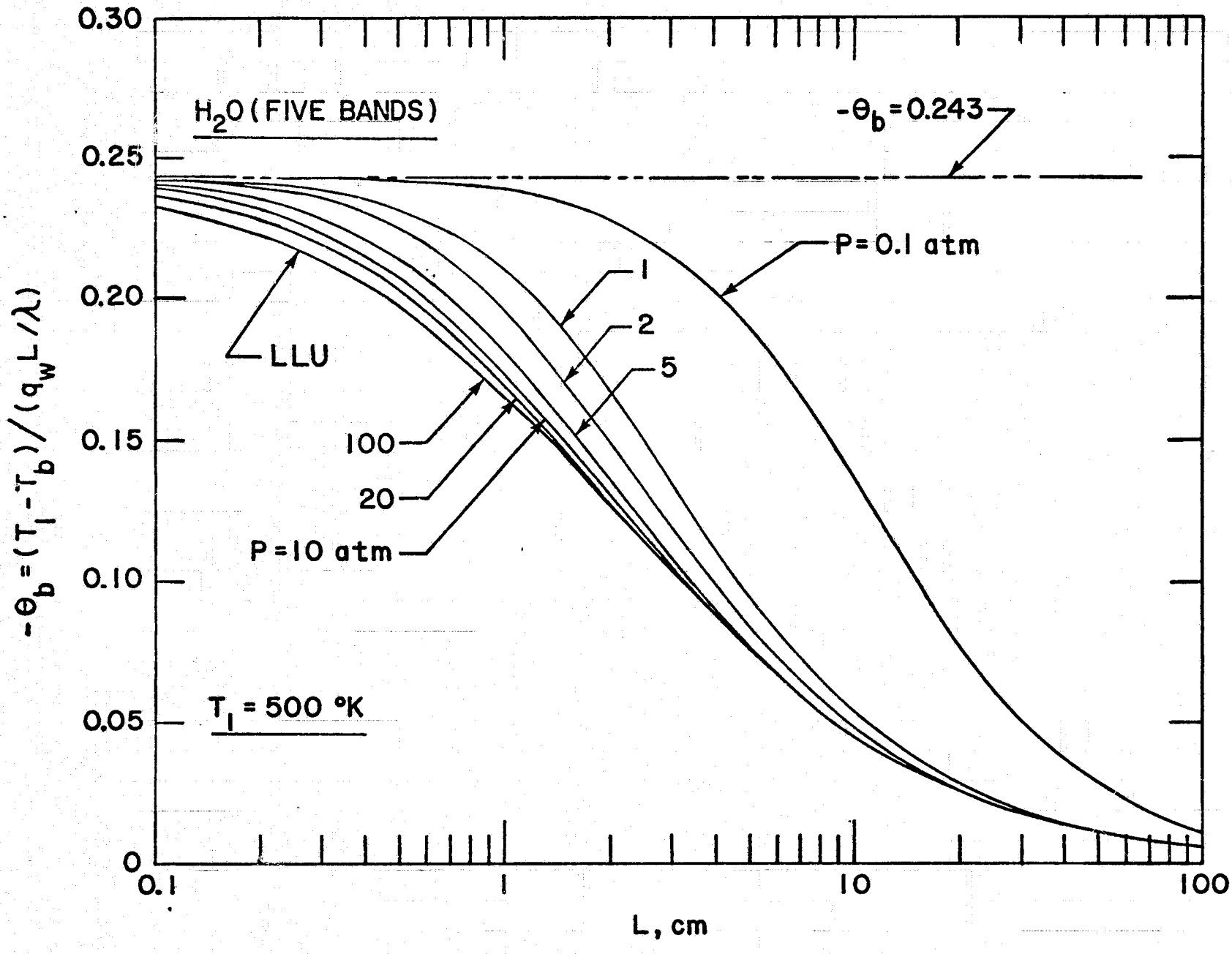

Fig. 3.8a Results for H_2O obtained by using the Tien and Lowder's correlation.

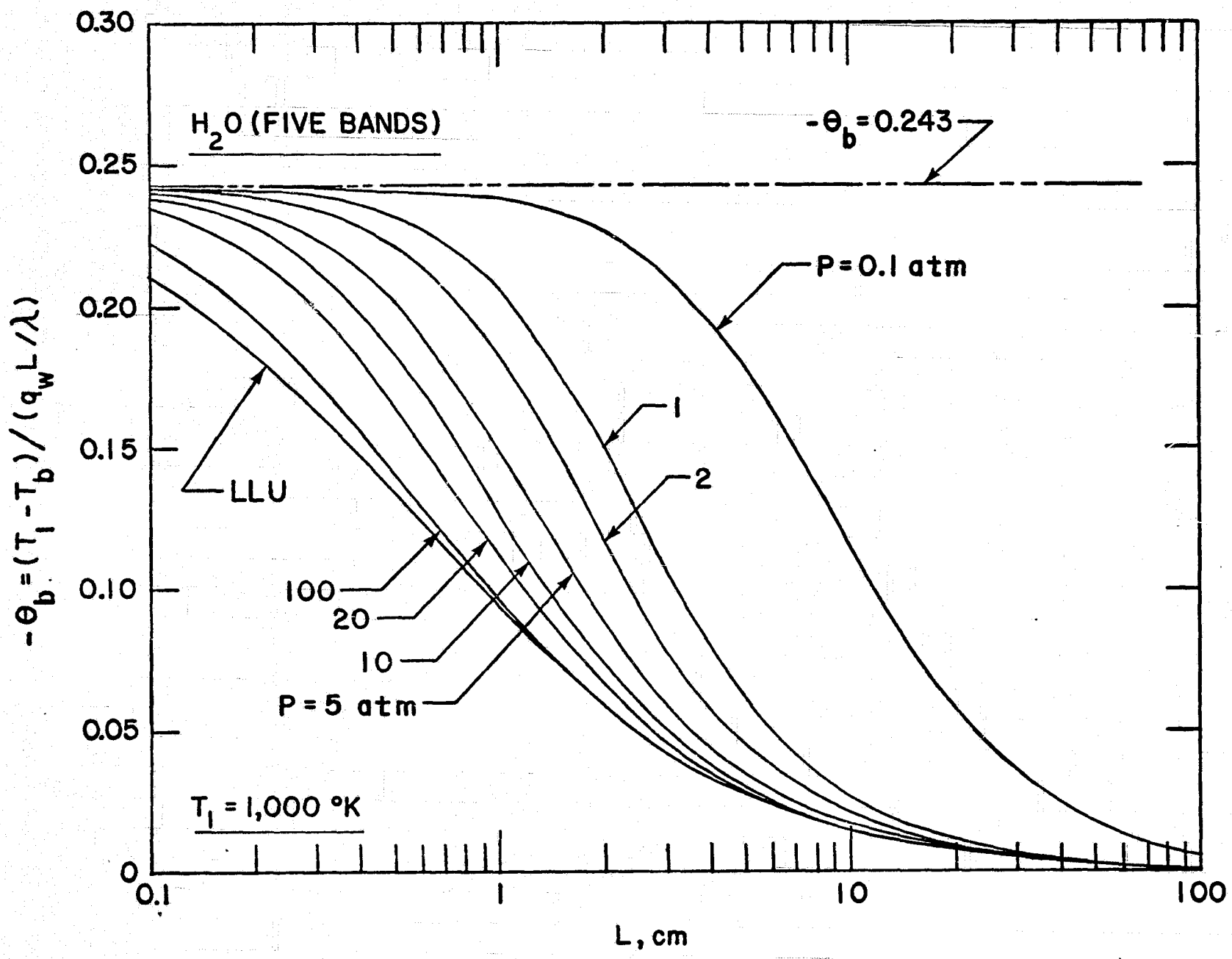

Fig. 3.8b Results for H_2O obtained by using the Tien and Lowder's correlation.

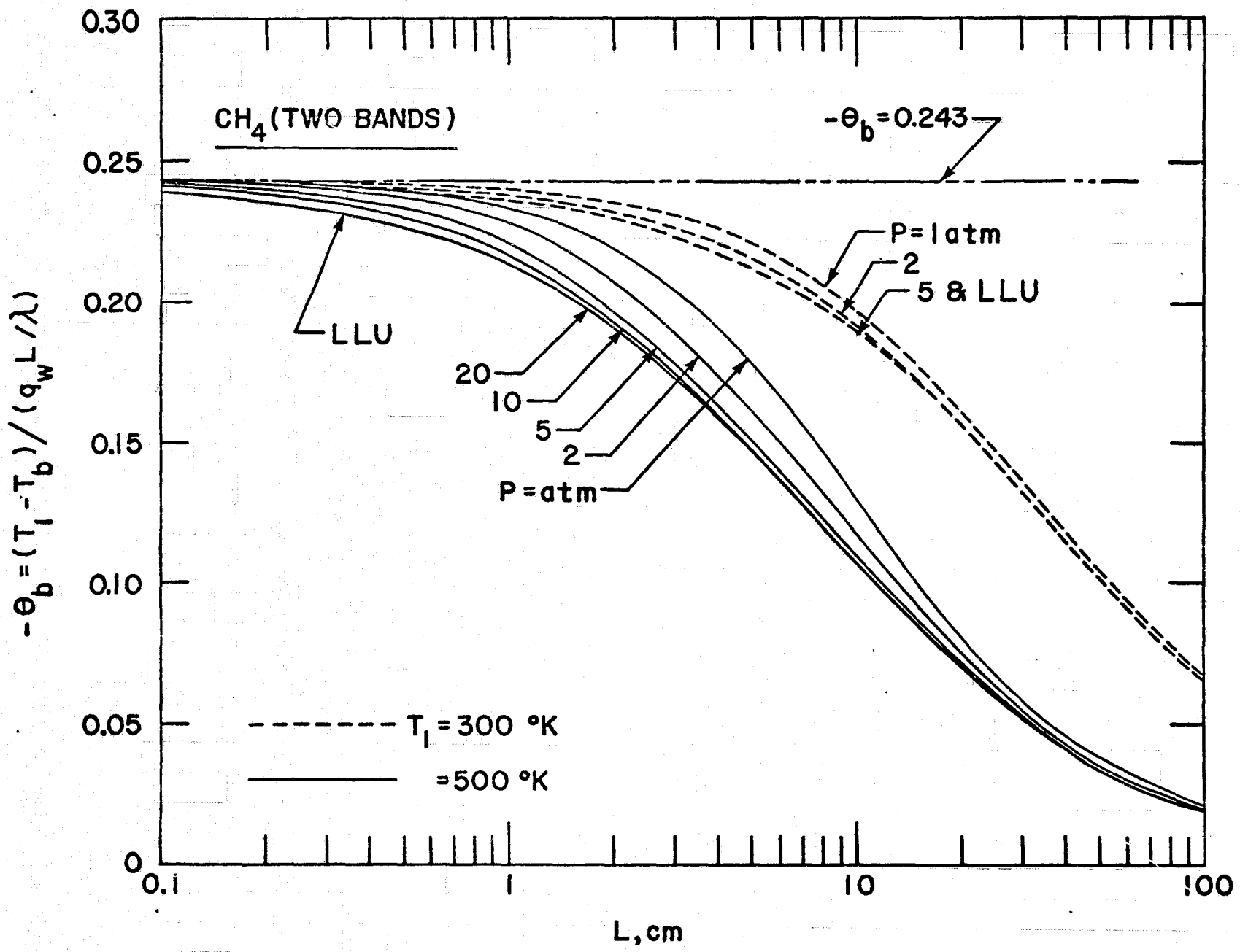

Fig. 3.9a Results for CH_4 obtained by using the Tien and Lowder's correlation.

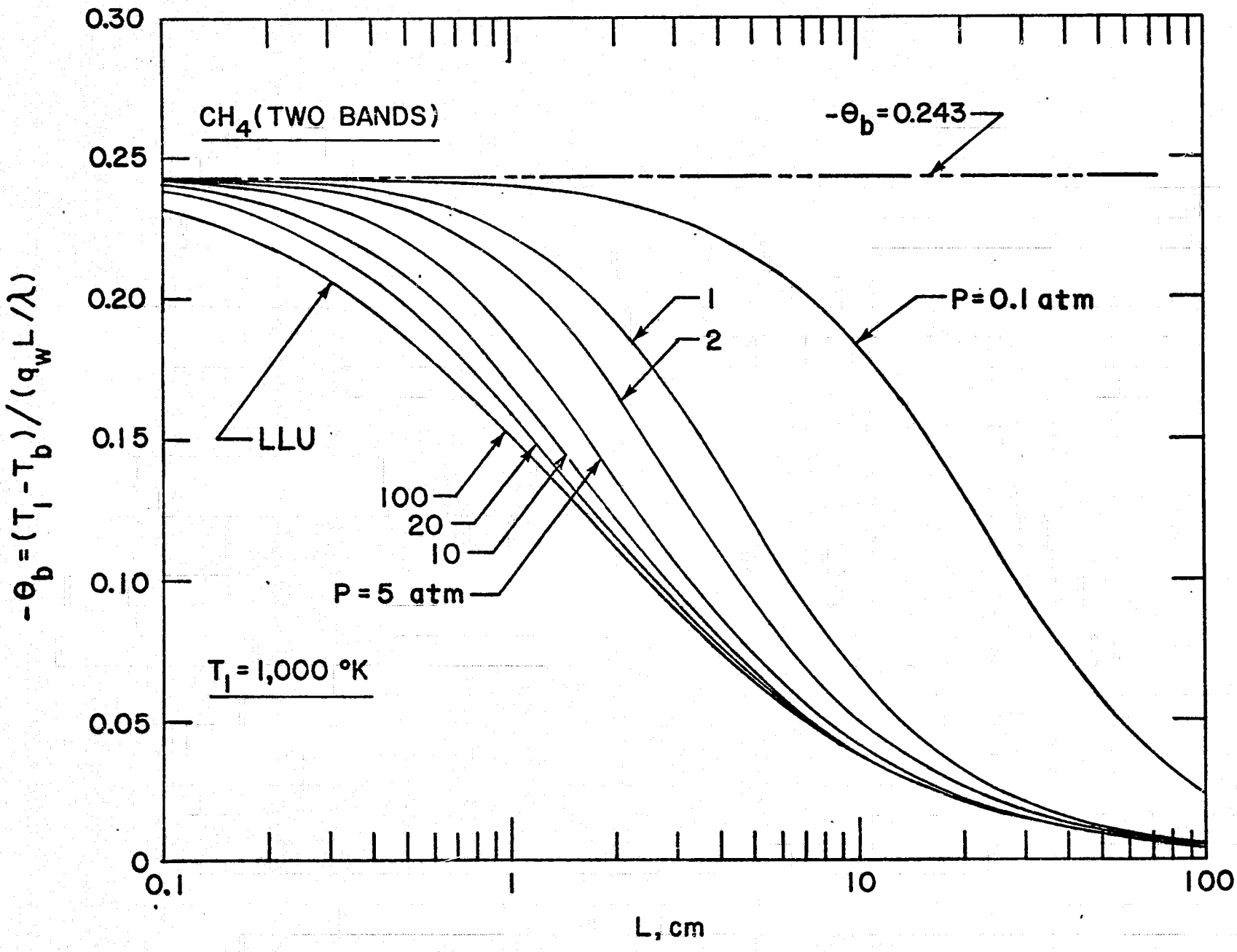

Fig. 3.9b Results for CH_4 obtained by using the Tien and Lowder's correlation.

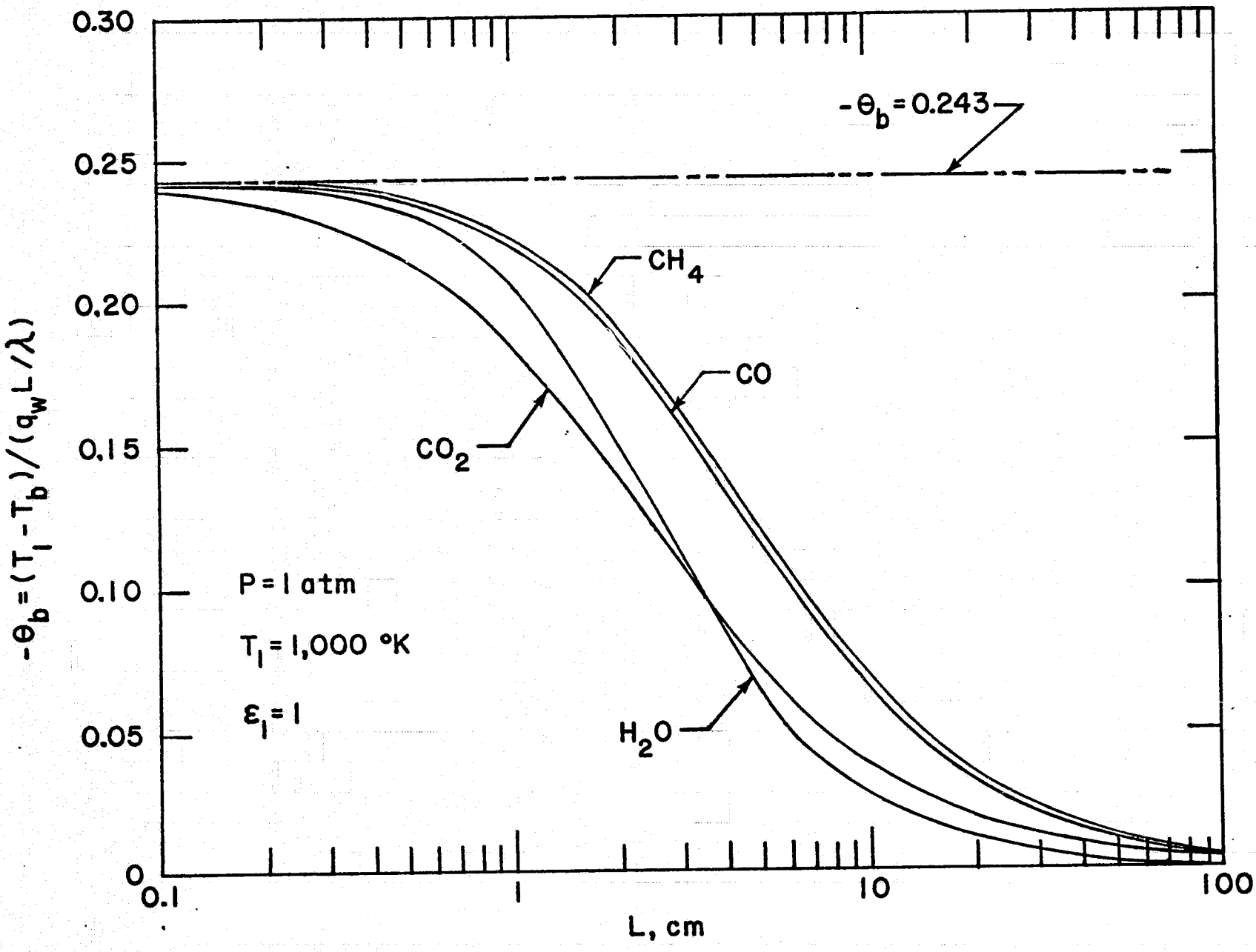

Fig. 3.10 Comparison of results of Tien and Lowder's correlation for T_l = 1,000 °K and P = 1 atm.

Bulk temperature results for CO (fundamental band) and CO_2 (15μ, 4.3μ, and 2.7μ bands) as obtained by employing the various correlations for band absorptance, are illustrated in Figs. 3.11 through 3.14. Results for CO are illustrated in Figs. 3.11 and 3.12 for wall temperatures of 500 °K and 1,000 °K respectively. It is evident from these figures that, except for the results of Tien and Lowder's correlation, results of other correlations differ from each other by less than 6% for all pressures and path lengths. For P = 0.1 and 1 atm, results differ by not more than 3%. The largest difference of about 6% occurs for P = 10.0 atm and T_1 = 1,000 °K. From a close observation of all the results presented in Figs. 3.11 and 3.12, it may be concluded that, for low to moderate pressures (say up to 5 atm), any one of the correlations (No. 2,3,5, or 6) could be employed in radiative transfer analyses. At high pressures, however, use of correlations 5 or 7 is recommended.

From Ref. [22] and the results presented in Figs. 3.6, it is noted that for CO the limit of large u_o is approached at P = 10 atm for T_1 = 500 °K and at 100 atm for T_1 = 1,000 °K. This trend is also evident, in general, from the results of Figs. 3.11 and 3.12. The results of Tien and Lowder's correlation, however, follow this trend more closely than any other result. As such, use of the Tien and Lowder's correlation is justified for radiative transfer analyses involving gases like CO (i.e., diatomic gases with single fundamental band having uniform distribution of spectral lines) at moderate and high pressures.

For CO_2, results of different correlations are illustrated in Figs. 3.13 and 3.14 for P = 0.01, 0.1, 1, and 10 atm, and for T_1 = 500 °K and 1,000 °K respectively. From Ref. [23] and the results presented in Fig. 3.7, it may be noted that for CO_2 the limit of large u_o (LLU) is approached at 2 atm for

T_1= 300 °K, at about 4 atm for T_1= 500 °K, and at about 10 atm for T_1=1,000 °K. Thus, results for 10 atm in Figs. 3.13 and 3.14 essentially are LLU results. For clarity, results of P = 1 and 10 atm are not plotted on the same graph.

As was the case with CO, the results of all correlations (except Tien and Lowder's) almost are identical for CO_2 also for P = 0.01 and 0.1 atm. This, however, would be expected because the low pressure (small β) situation corresponds to the case of square-root limit and most correlations are developed to satisfy this limit. It was pointed out earlier and in [12,14] that the square-root limit is not satisfied by the Tien and Lowder's correlation. At low pressures, therefore, use of the Tien and Lowder's correlation certainly is not justified. Other results of CO_2 (shown in Figs. 3.13 and 3.14) follow the same general trend as for CO in Figs. 3.11 and 3.12. The maximum difference between the results of different correlations is about 6% for P = 1 atm and T_1 = 1,000 °K. For the most part, results of correlations 3, 5, 6, and 7 are identical for P = 10 atm. This again would be expected because for CO_2, the LLU is approached at relatively lower pressures and most correlations are developed to satisfy the logarithmic limit. For gases like CO_2, therefore, use of any one of the correlations 2, 3, 5, and 6 is recommended at low and moderate pressures, and of 3, 5, 6, and 7 at high pressures. Use of the correlations 2, 3, 6, and 7, in a particular radiative transfer analysis, provides a greater mathematical flexibility and simplicity.

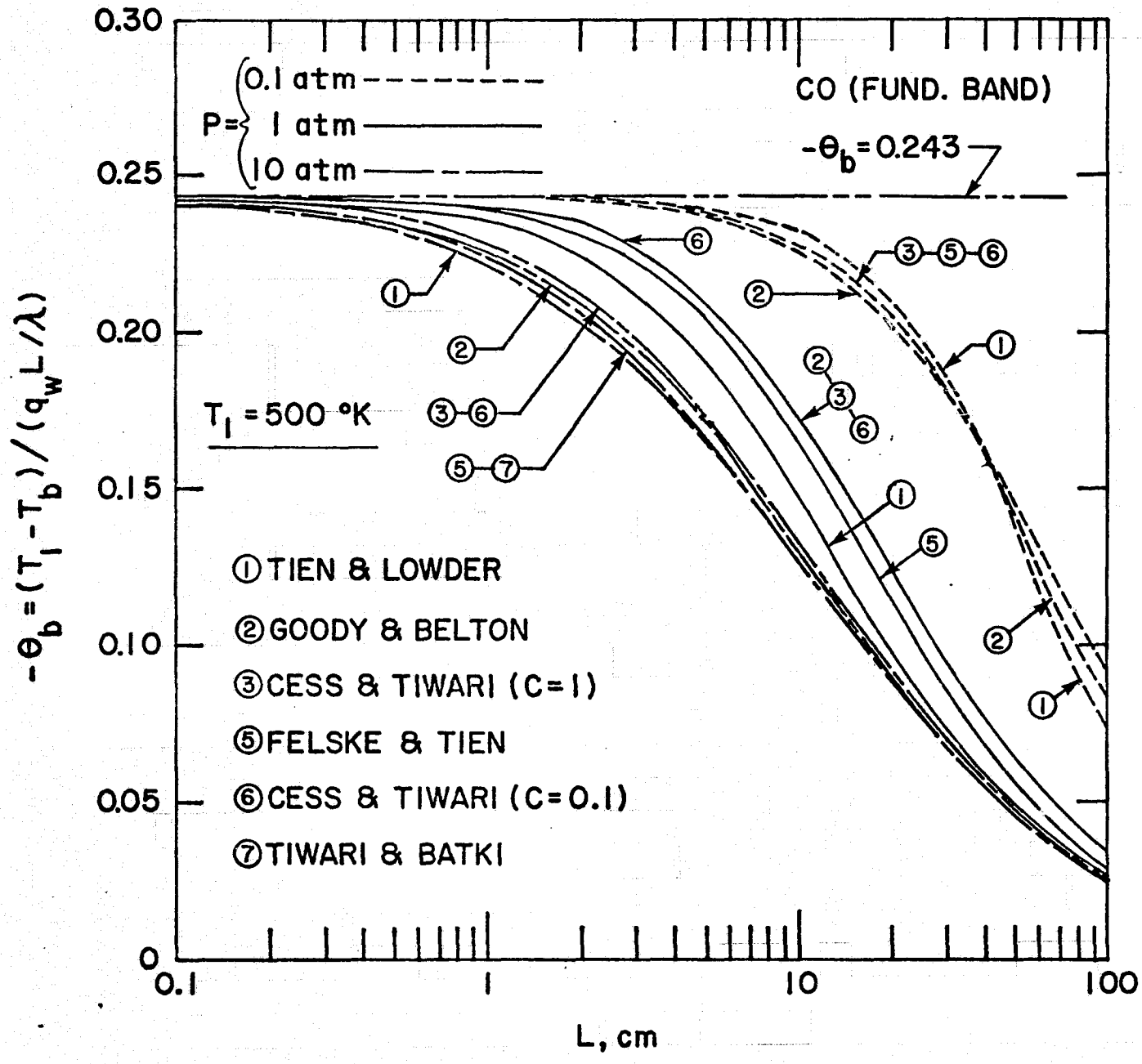

Fig. 3.11 Results for CO (fundamental band) with T_1 = 500 °K.

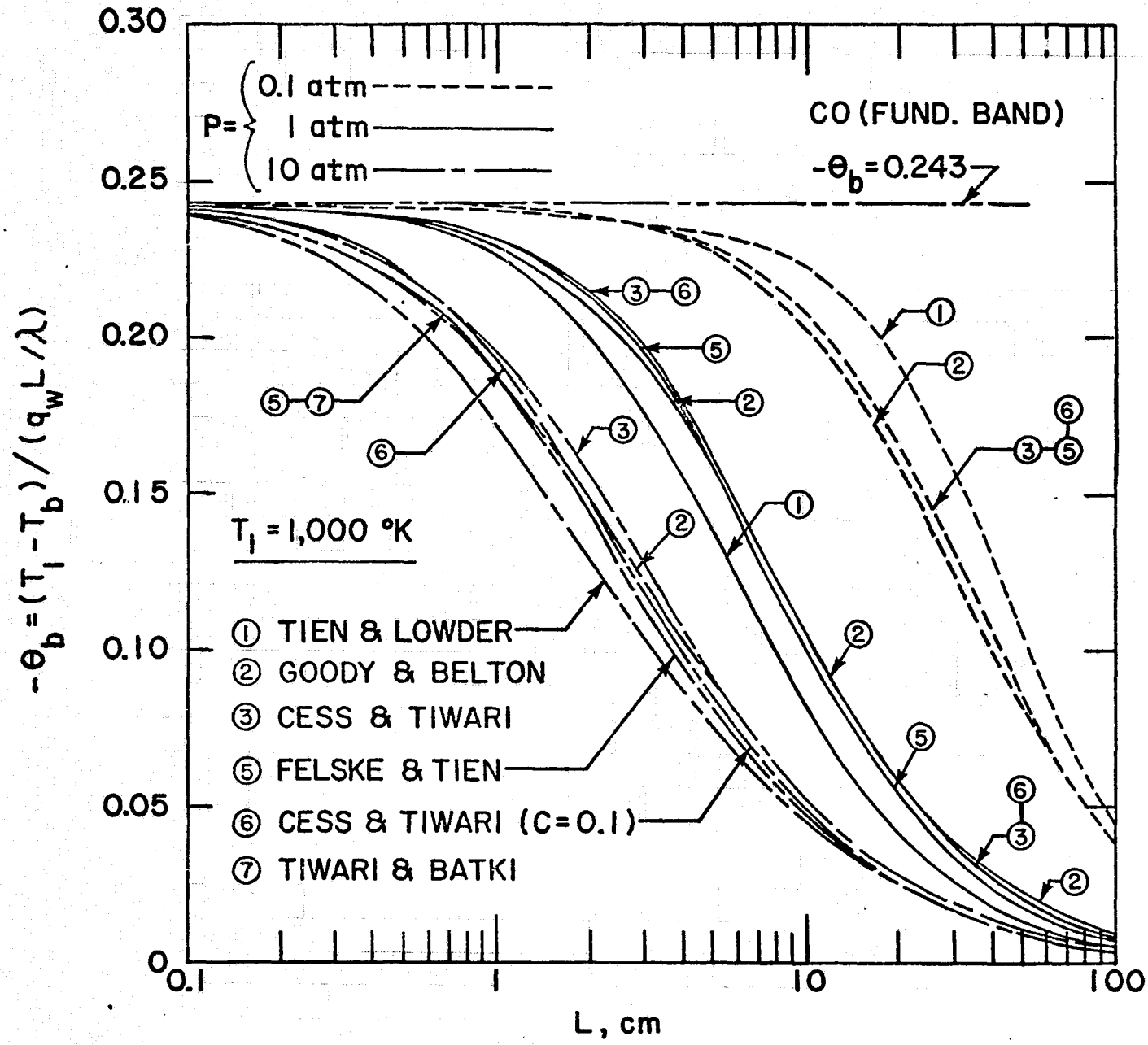

Fig. 3.12 Results for CO (fundamental band) with T_1 = 1,000 °K.

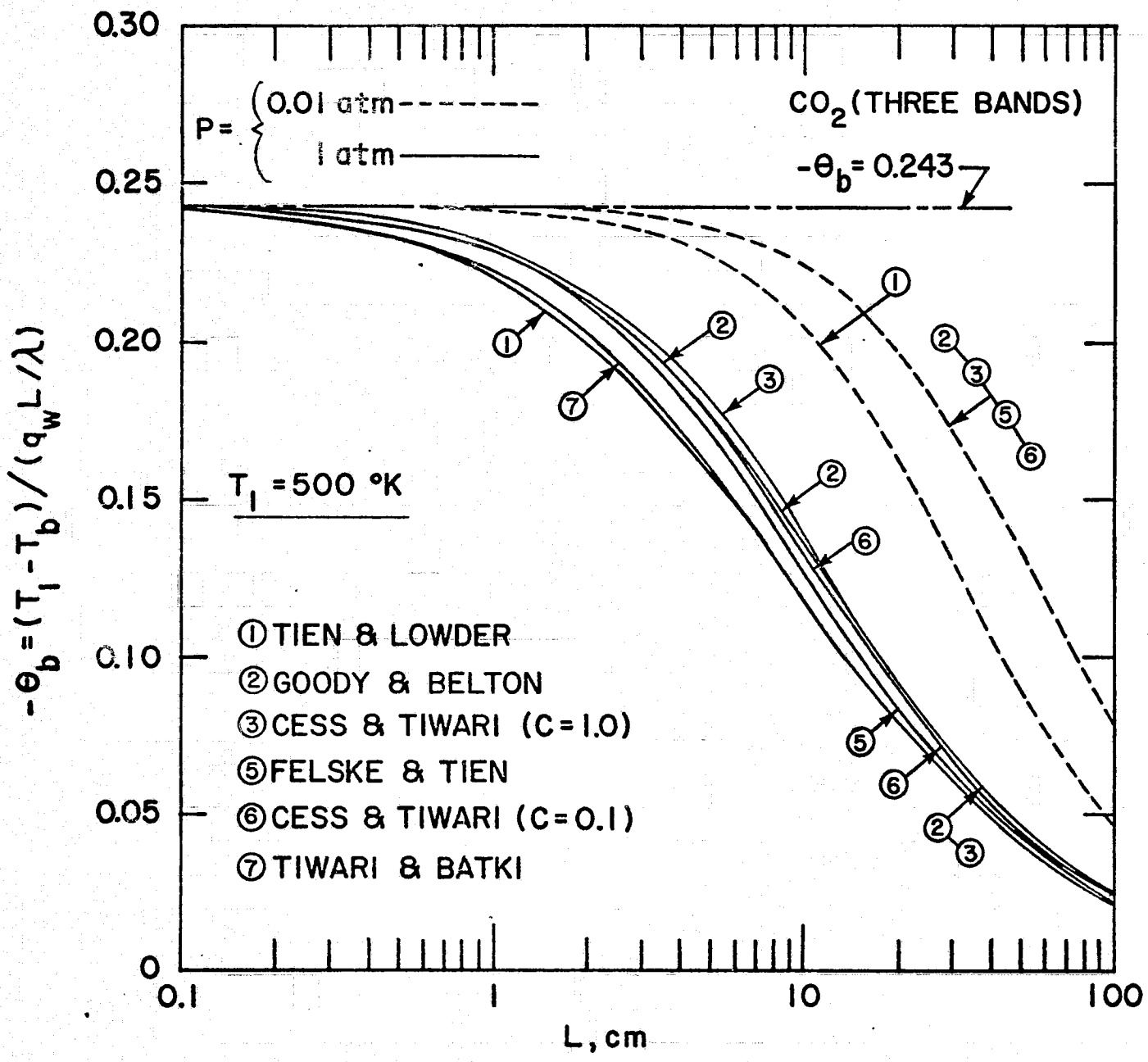

Fig. 3.13a Results for CO_2 (three bands) with T_1 = 500 °K.

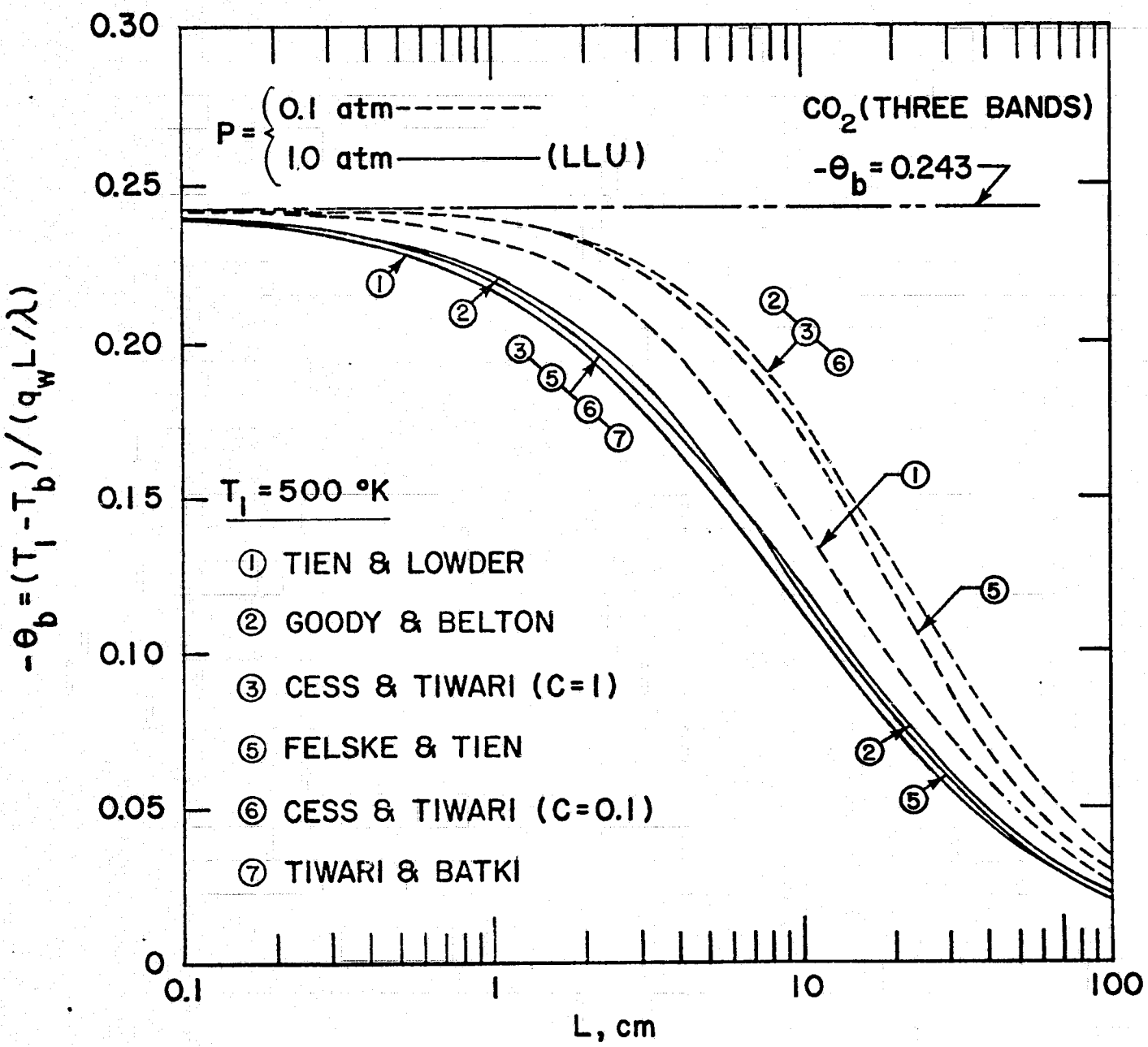

Fig. 3.13b Results for CO_2 (three bands) with T_1 = 500 °K.

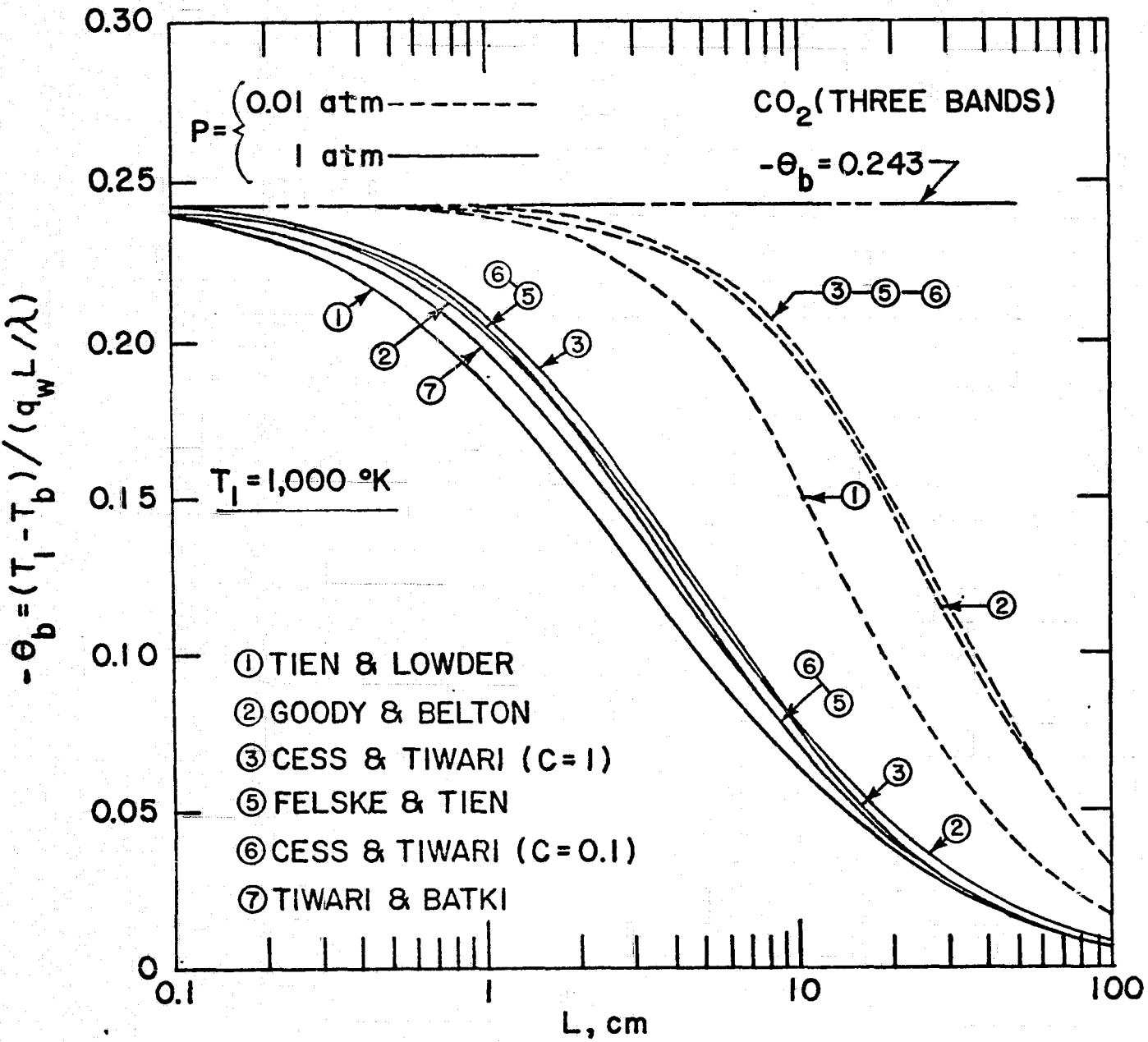

Fig. 3.14a Results for CO_2 (three bands) with T_1 = 1,000 °K.

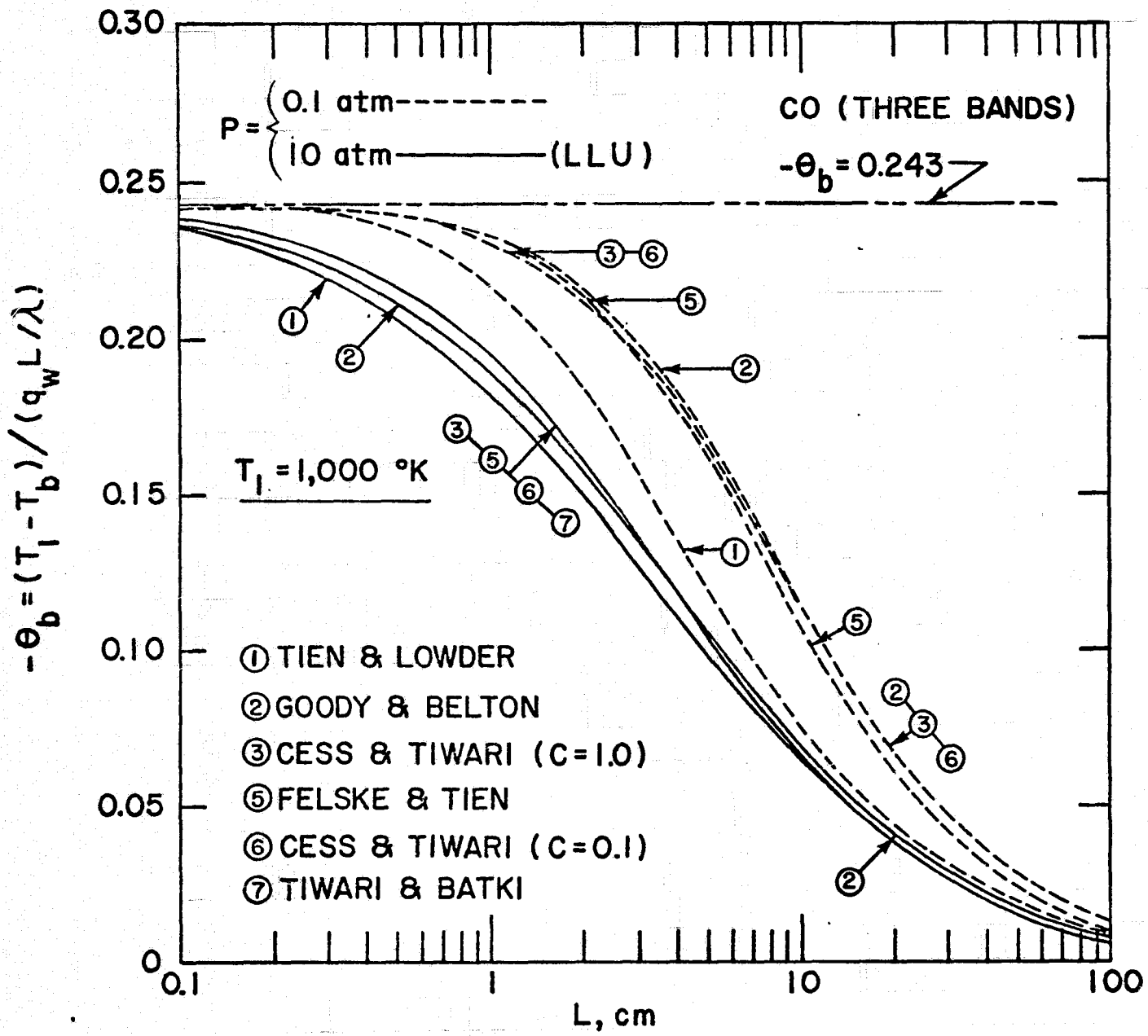

Fig. 3.14b Results for CO_2 (three bands) with T_1 = 1,000 °K.

CONCLUSIONS

In this study, use of several continuous correlations for total band absorptance were made to two problems to investigate their influence on the final results of actual radiative processes. For the case of radiative transfer in a gas with internal heat source, it was found that actual centerline temperature results obtained by using the different correlations follow the same general trend as the results of total band absorptance by these correlations. From these results, it may be concluded that use of the Tien and Lowder's correlation should be avoided at lower pressures, but its use is justified (at moderate and high pressures) to gases whose spectral behavior can be described by the regular Elsasser band model. For all pressures and path length conditions, use of the Cess and Tiwari's correlations could be made to gases with bands of highly overlapping lines. In a more realistic problem involving flow of an absorbing-emitting gas, results of different correlations (except the Tien and Lowder's correlation) differ from each other by less than 6% for all pressures and path lengths. Use of Tien and Lowder's correlations is justified for gases like CO at moderate and high pressures. For gases like CO_2, use of any other correlation is recommended. While Felske and Tien's correlation is useful for all pressures and path lengths to gases having random band structure, Tiwari and Batki's simple correlation could be employed to gases with regular or random band structure but for $P \geq 1.0$ atm.

REFERENCES

1. Elsasser, W. M., "Heat Transfer by Infrared Radiation in the Atmosphere," Harvard Meteorological Studies, No. 6, Harvard Univ. Press, Cambridge, Mass., 1942.
2. Kaplan, L. D., 1953 Proceedings of the Toronto Meteorological Conference, 1954, Royal Meteorological Society, p. 43.
3. Goody, R. M., Atmospheric Radiation I: Theoretical Basis, Oxford Univ. Press, London and New York, 1964.
4. Plass, G. N., "Models for Spectral Band Absorption," Journal of the Optical Society of America, Vol. 48, No. 10, Oct. 1958, pp. 690-703.
5. Plass, G. N., "Useful Representations for Measurements of Spectral Band Absorption," Journal of the Optical Society of America, Vol. 50, No. 9, Sept. 1960, pp. 868-875.
6. Wyatt, P. J., Stull, V. R., and Plass, G. N., "Quasi-Random Model of Band Abosrption," Journal of the Optical Society of America, Vol. 52, No. 11, Nov. 1962, pp. 1209-1217.
7. Edwards, D. K. and Menard, W. A., "Comparison of Methods for Correlation of Total Band Absorption," Applied Optics, Vol. 3, No. 5, May 1964, pp. 621-625.
8. Edwards, D. K., Glassen, L. K., Hauser, W. C., and Tuchscher, J. S., "Radiation Heat Transfer in Nonisothermal Nongray Gases," Journal of Heat Transfer, Vol. 89, Series C, No. 3, Aug. 1967, pp. 219-229.
9. Edwards, D. K. and Balakrishnan, A., "Thermal Radiation by Combustion Gases," International Journal of Heat and Mass Transfer, Vol. 16, No. 1, Jan. 1973, pp. 25-40.
10. Edwards, D. K. and Wassel, A. T., "The Radial Radiative Heat Flux in a Cylinder," Journal of Heat Transfer, Vol. 95, Series C, No. 2, May 1973, pp. 276-277.

11. Tien, C. L., "Thermal Radiation Properties of Gases," Advances in Heat Transfer, Vol. V, Academic Press, New York, 1968.

12. Cess, R. D. and Tiwari, S. N., "Infrared Radiative Energy Transfer in Gases," Advances in Heat Transfer, Vol. VIII, Academic Press, New York, 1972.

13. Tiwari, S. N., "Band Models and Correlations for Infrared Radiation," AIAA Paper 75-699, Presented at the AIAA 10th Thermophysics Conference, May 27-29, 1975, Denver, Colo. Also published in 1975-AIAA Progress in Astronautics and Aeronautics: Radiative Transfer and Thermal Control.

14. Tiwari, S. N. and Batki, R. R., "Infrared Band Models for Atmospheric Radiation," TR-75-T17, Nov. 1975, School of Engineering, Old Dominion University, Norfolk, Va.

15. Felske, J. D. and Tien, C. L., "A Theoretical Closed Form Expression for the Total Band Absorptance of Infrared-Radiating Gases," International Journal of Heat and Mass Transfer, Vol. 17, No. 1, Jan. 1974, pp. 155-158.

16. Goody, R. M. and Belton, M.J.S., "Radiative Relaxation Times for Mars (A Discussion of Martian Atmospheric Dynamics)," Planetary and Space Science, Vol. 15, No. 2, Feb. 1967, pp. 247-256.

17. Tien, C. L. and Ling, G. R., "On a Simple Correlation for Total Band Absorptance of Radiating Gases," International Journal of Heat and Mass Transfer, Vol. 12, No. 9, Sept. 1969, pp. 1179-1181.

18. Sparrow, E. M. and Cess, R. D., Radiation Heat Transfer, Brooks/Cole Publishing Co., Belmont, California, 1966.

19. Cess, R. D. and Tiwari, S. N., "The Large Path Length Limit for Infrared Gaseous Radiation," Applied Scientific Research, Vol. 19, Nov. 1968, pp. 439-449.

20. Cess, R. D. and Tiwari, S. N., "The Interaction of Thermal Conduction and Infrared Gaseous Radiation," Applied Scientific Research, Vol. 20, Jan. 1969, pp. 25-39.

21. Gille, J. C. and Goody, R. M., "Convection in a Radiating Gas," Journal of Fluid Mechanics, Vol. 20, Part 1, Sept. 1964, pp. 47-79.

22. Cess, R. D. and Tiwari, S. N., "Heat Transfer to Laminar Flow of an Absorbing-Emitting Gas Between Parallel Plates," TR-67-90, May 1967, College of Engineering, tate University of New York, Stony Brook, N. Y. Also published in Heat and Mass Transfer, Vol. 1 (Energy), Moscow, U.S.S.R., 1968.

23. Tiwari, S. N., "Infrared Radiative Energy Transfer in Nongray Gases," Ph.D. Dissertation, State University of New York, Stony Brook, N. Y., 1969.

24. Greif, R. and McEligot, D. M., "Thermally Developing Laminar Flows with Radiative Interaction Using the Total Band Absorptance Model," Applied Scientific Research, Vol. 25, Dec. 1971, pp. 234-244.

25. Echigo, R., Hasegawa, S., and Miyazaki, Y., "Composite Heat Transfer with Thermal Radiation in Non-Gray Medium-Part I Interaction of Radiation with Conduction," International Journal of Heat and Mass Transfer, Vol. 14, No. 12, Dec. 1971, pp. 2001-2015.

26. Donovan, T. E. and Greif, R., "Laminar Convection with an Absorbing and Emitting Gas," Applied Scientific Research, Vol. 31, No. 2, Aug. 1975, pp. 110-122.

27. Martin, J. K. and Hwang, C. C., "Combined Radiant and Convective Heat Transfer to Laminar Steam Flow Between Gray Parallel Plates with Uniform Heat Flux," Journal of Quantitative Spectroscopy and Radiative Transfer, Vol. 15, No. 12, Dec. 1975, pp. 1071-1081.